



저작자표시-비영리-변경금지 2.0 대한민국

이용자는 아래의 조건을 따르는 경우에 한하여 자유롭게

- 이 저작물을 복제, 배포, 전송, 전시, 공연 및 방송할 수 있습니다.

다음과 같은 조건을 따라야 합니다:



저작자표시. 귀하는 원저작자를 표시하여야 합니다.



비영리. 귀하는 이 저작물을 영리 목적으로 이용할 수 없습니다.



변경금지. 귀하는 이 저작물을 개작, 변형 또는 가공할 수 없습니다.

- 귀하는, 이 저작물의 재이용이나 배포의 경우, 이 저작물에 적용된 이용허락조건을 명확하게 나타내어야 합니다.
- 저작권자로부터 별도의 허가를 받으면 이러한 조건들은 적용되지 않습니다.

저작권법에 따른 이용자의 권리는 위의 내용에 의하여 영향을 받지 않습니다.

이것은 [이용허락규약\(Legal Code\)](#)을 이해하기 쉽게 요약한 것입니다.

[Disclaimer](#)

Thesis for the Degree of Master of Engineering

**An Automatic Hull Form
Generation and Multi-Objective
Approach for Optimization of Ship
Hull Forms**

by

May Thu Zaw

Department of Naval Architecture and Marine System
Engineering

The Graduate School

Pukyong National University

August 2018

**An Automatic Hull Form Generation and Multi-
Objective Approach for Optimization of Ship Hull
Forms**

**선형 자동 생성법과 다목적 최적화 기법을 이용한 선형
최적화**

Advisor: Prof. Dong Joon Kim

by

May Thu Zaw

A thesis submitted in partial fulfillment of the requirements

for the degree of

Master of Engineering

In Department of Naval Architecture and Marine Systems Engineering

The Graduate School

Pukyong National University

August 2018

**Automatic Hull Form Generation and Multi-Objective
Approach for Optimization of Ship Hull Forms**

A thesis

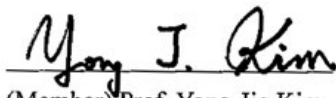
by
May Thu Zaw

Approved by:



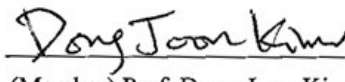
In-Chul Kim

(Chairman) Prof. In-Chul Kim



Yong J. Kim

(Member) Prof. Yong-Jig Kim



Dong Joon Kim

(Member) Prof. Dong-Joon Kim

August 2018

Contents

Abstract.....	iv
List of Figures.....	vi
List of Tables.....	viii
Chapter 1: Introduction.....	1
1.1 Background.....	1
1.2 Overview.....	2
1.3 Objective of study.....	4
1.4 Outline of Thesis.....	5
Chapter 2: Optimization Methods.....	6
2.1 Advanced Design Optimization Methods in Dakota.....	7
2.2 Brief Overview of Optimization Methods used in CAESES..	10
Chapter 3: Geometric Modelling.....	11
3.1 Parametric Modelling.....	11
3.2 Brief Overview of Parametric Modeling Techniques in CAESES.....	12
3.3 Partially Parametric Modelling Methods in CAESES.....	12
3.4 Free Form Deformation.....	14
3.5 Case Study.....	16
3.6 Remodeling of Bow and Stern of DTC hull to Parametric model.....	17
3.7 Selection of Design Parameters.....	21
Chapter 4: Computational Fluid Dynamics (CFD) Method.....	23
4.1 OpenFOAM Theoretical Background.....	23
4.2 Domain, Grids and Boundary conditions.....	25
4.3 Meshing.....	25
4.4 Use of InterFoam Solver.....	26
4.5 Validation of OpenFOAM results with Experimental Data...	28

Chapter 5: Optimization Process in Calm Water Condition.....	31
5.1 Design of Experiments.....	31
5.2 Software Connection.....	33
5.3 Single Objective Optimization.....	35
5.3.1 Case 1(Bow) - minimize total resistance at V=25 knots at design draft of 14.5m.....	35
5.3.2 Case 1(Stern)-minimize total resistance at V=25 knots at design draft of 14.5m.....	36
5.3.3 Case 2(Bow) - minimize total resistance at V=22 knots at design draft of 14.5m.....	37
5.3.4 Case 2(Stern) - minimize total resistance at V=22 knots at design draft of 14.5m.....	38
5.4 Multi-objective Optimization.....	39
5.4.1 Case 3(Bow) - minimize total resistance at V=22 knots and 25 knots at design draft of 14.5 m.....	41
5.4.2 Case 3(Stern) - minimize total resistance at V=22 knots and 25 knots at design draft of 14.5 m.....	42
Chapter 6: Results and Analysis.....	44
6.1 Analysis of Optimal Models at Different Operation Conditions.....	44
6.2 Optimal Model Selected from the Optimization in Calm Water.....	46
Chapter 7: Summary, Conclusion and Future Works.....	50
7.1 Summary.....	50
7.2 Conclusion.....	50
7.3 Future Works.....	51
Reference.....	52
국문요약.....	54

Acknowledgement..... 55
Appendix.....56



An Automatic Hull Form Generation and Multi-Objective Approach for
Optimization of Ship Hull Forms

May Thu Zaw

Department of Naval Architecture and Marine Systems Engineering
The Graduate School,
Pukyong National University

Abstract

Optimization is finding the solution with the most cost effective or highest achievable performance under the given constraints, by maximizing desired factors and minimizing undesired ones. Hull form optimization from a hydrodynamic performance point of view in calm water is important in preliminary ship design. The challenge of this work is getting a ship with lowest energy consumption in calm water by various optimization approaches to minimize the ship resistance at its given displacement and its service speeds. Different speeds were taken into account for the analysis of resistance performance of a vessel.

An academic container vessel (Duisburg Test Case developed and tested by the University of Duisburg-Essen) was taken for the study case. The parametric model of the vessel was developed by modifying the initial geometry with the use of CAESES 4.1.2. After getting a parametric model, it was simulated by OpenFOAM, the open Source code developed to validate with experimental results. After coupling OpenFOAM solver with CAESES, different optimization approaches were done by using CAESES/Dakota interface. The optimization was focused on the changes of the forward part of the vessel (bulbous bow)

and stern (underwater part).The optimal hull form was obtained in calm water condition by different optimization algorithms and was checked in different operation profiles. Finally, the results of the optimal hull form were compared with original design.

Keywords: Optimization, CFD, Multi-Objective, CAESES, OpenFOAM



List of Figures

Fig. 2.1 Automatic shape optimization loop.....	6
Fig. 2.2 Optimization framework using CAESES and OpenFOAM.	7
Fig. 2.3 Flow chart showing procedure of optimization process.....	8
Fig. 3.1 Geometry deformed by free form deformation method.....	16
Fig. 3.2 DTC hull 3D model.....	16
Fig. 3.3 B-spline control box and bulbous bow of the model.....	18
Fig. 3.4 Parametric modelling of bulbous bow using control B spline box.....	19
Fig. 3.5 Initial surface and new sections after free form deformation.....	19
Fig. 3.6 Parametric modelling of stern using control B spline box...	20
Fig. 3.7 Initial profile of stern and new profile after free form deformation	20
Fig. 4.1 CFD computation steps.....	24
Fig. 4.2 Domain grid and boundary conditions set up.....	25
Fig. 4.3 Meshing(Refinement) using SnappyHexMesh.....	26
Fig. 4.4 Mesh domain filled with water (red) and air (blue).....	26
Fig. 4.5 Convergence history of the DTC hull at 25knots.....	27
Fig. 4.6 Flow pattern around the DTC hull.....	28
Fig. 4.7 Comparison of numerical result from OpenFOAM and experimental data from HAVA towing tank.....	30
Fig. 5.1 Surrogate based optimization process.....	32
Fig. 5.2 Software connector interface.....	34
Fig. 5.3 Single objective optimization of bow at 25 knots.....	36
Fig. 5.4 Single objective optimization of stern at 25 knots.....	37
Fig. 5.5 Single objective optimization of bow at 22 knots.....	38
Fig. 5.6 Single objective optimization of stern at 22 knots.....	39

Fig. 5.7 Multi-Objective optimization of bow (MOGA) 42

Fig. 5.8 Multi-Objective optimization of stern (MOGA) 42

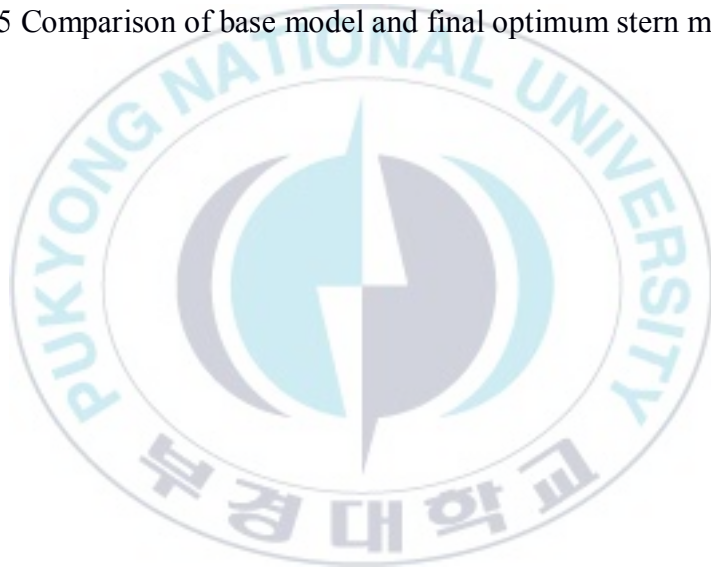
Fig. 6.1 Comparison of resistance base model and Optimum for
different operation condition..... 47

Fig. 6.2 Comparison of wave contour of base model and final
optimum model.....47

Fig. 6.3 Comparison of wave profile of base model and final
optimum model..... 48

Fig. 6.4 Comparison of base model and final optimum bow model..48

Fig. 6.5 Comparison of base model and final optimum stern model.49



List of Tables

Table 3.1 Main dimensions of DTC in design loading conditions...	17
Table 3.2 Design variable and % difference to original.....	22
Table 4.1 Results of resistance model tests.....	29
Table 4.2 Results and comparison of base model simulations in OpenFOAM.....	29
Table 5.1 Comparison of base design and optimized bow at 25 knots.....	35
Table 5.2 Comparison of base design and optimized stern at 25 knots.....	36
Table 5.3 Comparison of base design and optimized bow at 22 knots.....	37
Table 5.4 Comparison of base design and optimized stern at 22 knots.....	38
Table 5.5 Comparison of base design and optimized bow at two speed (multi-objective).....	41
Table 5.6 Comparison of base design and optimized stern at two speed (multi-objective).....	43
Table 6.1 Number of CFD run for each case.....	44
Table 6.2 Comparison of base design and optimized design for each case.....	45
Table 6.3 Total resistance (N) for selected optimal models at different operation condition.....	46
Table 6.4 Total resistance % difference for selected optimal models at different operation condition.....	46
Table 6.5 Geometry variation trend of optimized bulbous bow	49
Table 6.6 Geometry variation trend of optimized stern	49

Chapter 1: Introduction

1.1 Background

Green ship technologies are considered as an importance in diverse areas of ship design. As carbon dioxide emission are increasing, shipbuilding industries are trying to develop new design concepts and technologies towards fuel economic ship design including use of new technology devices and renewable energy sources. Hydrodynamic optimal shape designs are one of component of to achieve fuel economic design, although the reduction percentage of CO₂ emission can be achieved 2–3% maximum. However, it is not negligible because hull form design is a starting point of the new shipbuilding process and it has great influences on resistance and propulsion performance. In addition to its hydrodynamic effects, hull form design has influences on costs and performance. In order to reduce costs and improve the performance, ship design must need new concepts and multi-criteria optimized ships. Therefore researcher and design team has been developed simulation-based design optimization (SBDO) methods, to generate automatic hull variants and optimize their hydrodynamic performance, combining resistance and motion solvers, design modification tools, and different kinds optimization algorithms as well as multi-objective. In order to reduce costs, it is important to get the minimum resistance for the ship. The resistance of a ship at a given speed is the force required to move the ship at that speed through calm water. Ship resistance estimation is a complicated task. Resistance can be divided down into frictional and residual components. There are three different methods to predict ship resistance: empirical methods, model testing and numerical simulations. The most effective and efficient one

is numerical methods. Nowadays there are lots of commercial software to predict the resistance numerically.

The ship design process is often under the control of geometric modeling. Next, the model performance is analyzed with various methods. If the result is not satisfactory, the iterative steps are repeated until the desired performance is obtained. If the resistance requirements are not met, modification of the hull form is made and another model test is performed. This process is called a system for “manual optimization”. In recent years computational methods (CFD) have been developed and widely used in the design process to predict the flow around the hull and the resistance of the hull. Different design parameters may be compared based on computed results and the best one is then selected for proceeding next steps. In this way CFD methods may help to speed up the “manual optimization” process by reducing “iterations” number to find the final shape which can also save time, cost and energy. In here a CFD method and a mathematical optimization method together with a program for hull form variation is coupled together within a framework. This system can then be used to find a hull form that is optimized with respect to properties computed by the CFD method, like the resistance, maximum wave height, velocity in the propeller plane, etc. One or more constraints, for instance displacement and hull main dimensions, must then be introduced to limit the modifications of the hull. This is called a system for “automatic optimization” [1].

1.2 Overview

The hydrodynamic performance of a hull form in calm water is a major aspect for a naval architect in preliminary design stage. In the past, ships are designed based on the performance in calm water condition and there are many

attempts to optimize the calm water resistance of the vessel by varying form parameters. In the optimization process, the SIMPLEX algorithm or genetic algorithm is linked to the computational method to obtain an optimum hull form by several geometrical constraints such as internal fitting, displacement and stability.

There are different kinds of approaches to study hydrodynamic performance which are (a) the empirical approach that is in the form of constants, formula and curves developed from the parent ship or similar shapes, (b) the experimental approach that is the testing of a scaled model of original hull form and analyzing the performances, expanding to full scale results and (c) the numerical approach that has become increasingly important for ship resistance and powering. Therefore, ship optimization based on CFD simulation becomes the major factor of developing new optimal ship hull forms by minimizing ship resistance. Reducing the resistance leads to less consumable power, less emissions and noises [2].

The optimization process is fully automated requiring no user interaction. In this thesis, the steady wave system of a ship moving through calm water is approximated by means of CFD (Computational Fluid Dynamics) simulation applying OpenFOAM. The modelling of the geometry of the initial design, the coupling of the CFD solver and performing the optimization process to minimize the wave-making resistance were done by the use of CAESES developed by FRIENDSHIP SYSTEMS [3].

Ship hull form optimization offers several benefits: in the way of:

- Better understanding of the design task (and the design space),
- Creating design with superior performance (and better trade-offs),

- Allowing shorter time-to-market (and faster response to market changes),
- Reducing risk (and building confidence),
- Saving costs (and avoiding expensive late changes).

Hull form optimization is conducted both for investigating new ideas and possibilities at the initial design stage and for fine-tuning of a given design at a later stage when only small changes are still acceptable.

1.3 Objective of Study

The main objective of this thesis is to study the approaches for the optimization of fore body (bulbous bow) and stern of the hull (underwater part) form of a container vessel. In this thesis, an automated hull form variation methodology is developed based Simulation Driven Design method with using new generation of designs, analysis with CFD solver and optimization software combination. The optimization process was focused on minimizing the resistance of the vessel in calm water. For this purpose, parametric modeling software CAESES (FRIENDSHIP-FRAMEWORK) was used to build the optimization process under one software and handle the process automatically. CAESES itself has no CFD solver and it was needed to couple with external CFD solver. Furthermore, the coupling of OpenFOAM with CAESES to check the resistances considering different scenarios of different speeds had done.

The fore body and aft body of the hull form was modelled as partial parametric model in CAESES and it was simulated with CFD solver OpenFOAM. The optimization process was connected with CAESES/Dakota Interface to get the parameter variation .The full set-up optimization in

CAESES process permits to get the best hull form for resistance. After optimization, initial and optimum hull forms were compared to show that how to improve resistance with some local parameters.

1.4 Outline of the Thesis

The research was divided into 7 Chapters. The general contents of each chapter can be summarized as follows:

Chapter I *Introduction*: This chapter is the history and the background of the ship design process and general methods of hull form optimization is presented.

Chapter II *Optimization Methods*: This chapter explains different kinds of algorithms and the pros and cons of each method.

Chapter III *Geometric Modelling*: Here the geometry variation method is presented in details.

Chapter IV *Computation Fluid Dynamics Method*: This chapter presents the theory and usage of CFD solver OpenFOAM. The OpenFOAM results and Experimental results are compared in this chapter.

Chapter V *Optimization Process*: This chapter presents the optimization process under the Framework of CAESES. Different Optimization process and multi-objective optimization approach is performed in here

Chapter VI *Results and Analysis*: This chapter contains all the results contents obtained from simulation and analysis of the result and explanation is included.

Chapter VII *Summary, Conclusions and Recommendations*: This chapter contains the conclusion and summary of the whole optimization procedure in this thesis.

Chapter 2: Optimization Methods

Automatic shape optimization has gained popularity these days in various industrial sectors. As the performance of a flow-exposed object can be achieved accurately with CFD (Computational Fluid Dynamics) method, even small changes in design can be analyzed and captured. Fig. 2.1 shows the automatic shape optimization loop.

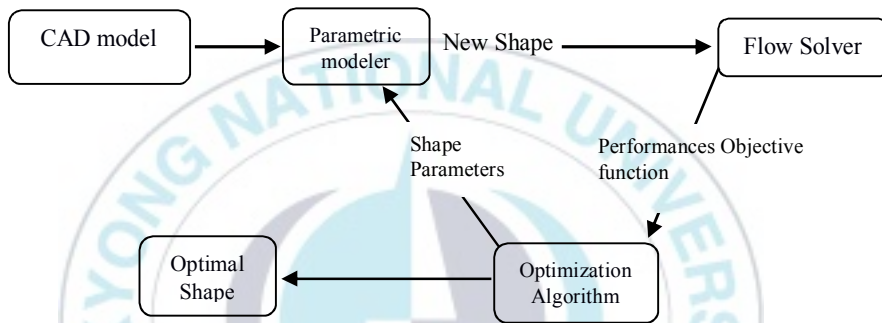


Fig. 2.1 Automatic shape optimization loop

Different types of tools were connected together to perform an automatic shape optimization such as a parametric modeler, a meshing and flow solver to calculate numerical calculations and an optimization algorithm to change the parameter to be able to find optimal one. Recent technological progresses allow to automatically run the meshing, the CFD flow solver and the post-processing (GUI) of the relevant results of the computation but less efforts had been dedicated to the development of efficient parametric modelers. The parametric modeler deforms the geometry according to the optimization algorithm output. It is important to get possible shapes to be explored. To be like this, the parametric modeler was needed to modify the shape of the geometry using a reduced number of parameters. It is necessary to provide a precise control of the geometry to generate a wide range of feasible shapes. In

this work, a new approach was proposed to shape deformation for parametric modelers with the purpose of being in targeted into an automatic shape optimization loop with a CFD solver.

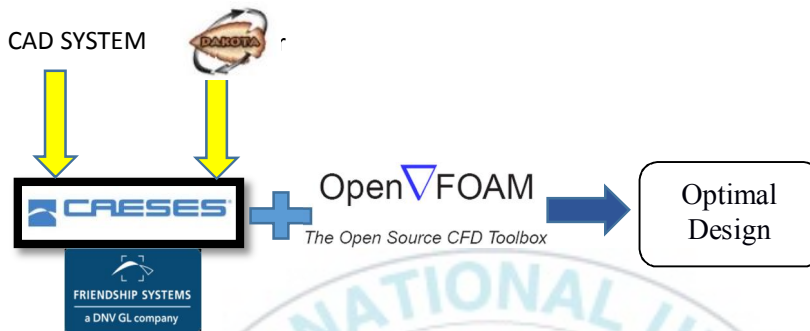


Fig. 2.2 Optimization framework using CAESES and OpenFOAM

2.1 Advanced Design Optimization Methods in Dakota

The free optimization toolkit Dakota (from Sandia National Labs) have developed an easy-to-use CAESES[®] interfaces with it. The full method set of Dakota can be applied directly within the CAESES[®] GUI. This includes advanced sampling techniques and strategies e.g. for robust design optimization including surrogate models. Different kinds of “meta-algorithm” capabilities have been described below [4].

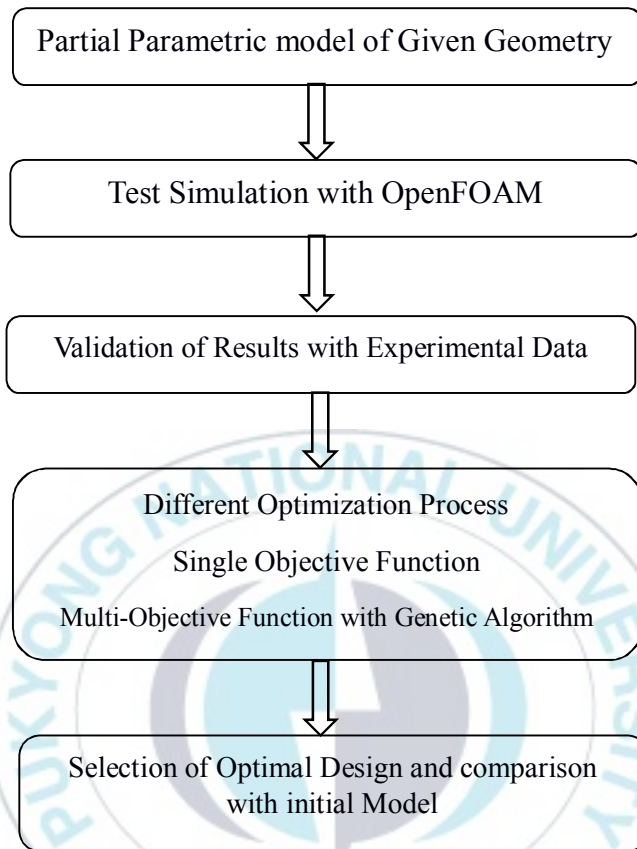


Fig.2.3 Flow chart showing procedure of optimization process

- (i) **Hybrid minimization:** In this method, a sequence of minimization methods are applied to find an optimal value. This method is capable to exploit the strengths of different minimization algorithms through different stages of the minimization process.
- (ii) **Multi-start Local Minimization:** A simple, heuristic, global minimization technique is to use many local minimization runs, each of which is started from a different initial point in the parameter space. This is known as multi-start local minimization. This is an attractive method in situations where multiple local

optima are known or expected to exist in the parameter space. Since solutions for different starting points are independent, parallel computing may be used to concurrently run the local minimizations.

- (iii) **Pareto Optimization:** In the Pareto optimization method, multiple sets of multi-objective weightings are evaluated. Dakota performs one multi-objective optimization problem for each set of multi-objective weights. The collection of computed optimal solutions form a Pareto set, which can be useful in making trade-off decisions in engineering design. Since solutions for different multi-objective weights are independent, parallel computing may be used to concurrently execute the multi-objective optimization problems.
- (iv) **Surrogate-Based Minimization:** Surrogate models approximate an original, high fidelity “truth” model, typically at reduced computational cost. In the context of minimization (optimization or calibration), surrogate models can speed convergence by reducing function evaluation cost or smoothing noisy response functions.
- (v) **Multi-Objective Genetic Algorithms:** Genetic Algorithm is inspired by the evolution theory by means of a process that is known as the natural selection and the ‘survival of the fittest’ principle. The common idea behind this technique is similar to the other evolutionary theory: consider a population of individuals; the environmental pressure causes natural selection which leads to an increase in the fittest of the population. It is easy to see such a process as optimization. In this thesis, the optimization toolkit

Dakota coupled with CAESES will be used for different optimization approaches.

2.2 Brief Overview of Optimization Methods used in CAESES

The following two methods are the surrogate based optimization methods coupled with CAESES as pre-configured input templates.

- (a) **Local Optimization Efficient-** Internally, this method creates a surrogate model (response surface) and conducts a local optimization on this model. For the initial surrogate model, existing point data can be used e.g. from a previous sensitivity analysis. During the run, the surrogate model is iteratively fine-tuned: the optimum design from the local search is evaluated and the information is added to the surrogate model – which step by step increases the quality of the model.
- (b) **MOGA Global Optimization Efficient-** In this method, a MOGA is conducted on a surrogate model that is iteratively built-up. For the initial model, data from a previous run (e.g. sensitivity analysis) can be recycled as well. With this approach, the method might be suitable even for rather expensive evaluations.

The author studied a lot of reference works for optimization of hull forms for resistance and different optimization algorithms and in this thesis will be focused on this specific work by the use of OpenFOAM solver, coupling with CAESES.

Chapter 3: Geometric Modelling

3.1 Parametric Modelling

In order to start optimization process, firstly the geometry was needed to modify. This process play an important role in the optimization loop. Because form variations consist of not only changing the parameters but also requires to provide some constraints like constant displacement, surface smoothness, etc. Most widely used and most simplex method of generating hull shape parameters is the fitting of discrete ship offset data with parametric representations such as polynomials, cubic, and Bezier and B-Spline curves or surfaces. To modify the shape, the hull offset data and control points, are directly used as design variables .The advantage of this method is ease of flexibility in controlling each control point but results in less efficient because the high degree of freedom in control points variations can cause deviations from the desired shape. Nowadays, there are lots of CAD software systems in the market and among them AutoCAD, Rhinoceros and Solidworks are famous. Solidworks and Rhinoceros (with Grasshopper plugin) can handle parametric modeling. In here, CAESES developed by FRIENDSHIP SYSTEM is used as a CAD modeling and a software connector and DAKOTA (developed by Scania University) is used as an optimizer.

Zhang et al (2008) studied on “Parametric Approach to Design of Hull Forms” [1] .This paper was about the parametric modelling of the hull form with the use of form parameters and the longitudinal function curves and combining the parametric approach to CFD method for optimization. Parameters mainly used for the manipulation of wave resistance are relative with the shape of bulbous bow and stern.

3.2 Brief Overview of Parametric Modelling Techniques in CAESES

CAESES is a powerful and flexible parametric 3D modeler. Unlike the others tool, the main focus of CAESES is the smart design and robust variation of geometry surfaces. CAESES enables the powerful surface generation tools to create an efficient variable geometry model for optimization [5].

- (a) **Fully-parametric modelling:** In fully parametric modelling, the entire shape is defined by a set of parameters. Some parameters may be at a high level like the length, width and height of a vessel. Other parameters may determine details like an entrance angle at a particular location. Typically, many parameters are set relative to or as combinations of other parameters. For optimization, fully-parametric modeling is very powerful since it enables both local and global changes in the early design phase and small adjustments when fine-tuning at a later point in time.
- (b) **Partially parametric modelling.** In partially-parametric modelling, only the local changes to an existing shape are defined by parameters while the undesired parts are fixed. Partially-parametric models are usually quick and fairly easy to set up. When compared to fully-parametric models they typically contain less knowledge (intelligence) about the product. In general, it is more difficult to excite large modifications compared to fully parametric. After all, the new shapes are derived from the baseline and, thus, cannot look totally different. Still, they are well suited for fine-tuning without much overhead.

3.3 Partially Parametric modeling methods in CAESES

The method presented here has the ability to deform geometry of the existing geometry. Directly moving the control points of the NURBS surface

mainly used in CAD software to generate new shapes was not appropriate. As the number of control points to represent adequately the shape may be too large (3 degrees of freedom per control point) to be used in shape optimization, the possibility of the undesired shape is high. Another difficulty is complex geometry models that is built with trimmed, or subdivided into numerous patches cannot be deformed in a structured way and they are not clean enough for CFD computations. For CFD computation, the object geometry is represented by a mesh representation. The deforming method presented in this thesis can be used on both surface and mesh representations of shapes. This is focused on reducing the number of degrees of freedom of the deformation problem. It is introduced a physical and a design meaning into the optimization process, allowing also to generate a majority of shapes that are valid. Shape deformation of ships forms for automatic shape optimization is a relatively recent approach. Firstly, Free Form Deformation (FFD) and morphing are classical methods created for 3D animation purposes, and later they can also been applied to shape optimization for ships. As these technique are specially intended to shape deformation, it is more effective than the traditional deformation ways like changing the control point of the surface FFD methods are very efficient and a small number of degrees of freedom is necessary to control the whole shape of the object. However, for the detail local deformation, the number of control points are needed to increase by refining the areas of interest. The exploration of the space of possible optimal shapes can be reduced effectively.

3.4 Free Form Deformation

Free Form Deformation techniques help to quickly optimize existing geometry. With this additional capabilities, CAESES focuses on CFD engineers that want to import and reshape their design with regards to the flow performance. FRIENDSHIP SYSTEMS provide the first version of its freeform deformation, greatly complementing the existing shift transformation of CAESES. This new functionality allows users of CAESES to easily deform imported CAD geometries and CAE data such as volume meshes. Naturally, the design variables of such a user defined transformation can be controlled by the variation and optimization engines of CAESES, for conducting fully-automated shape studies.

For the parametric deformations two tools had been created, described below. Volume deformation (also called global or free form deformation) was made by defining a box around the part of the hull form to be modified, e.g. the complete fore body or the stern. This immediately removes the problem of how to describe a hull form with a limited set of parameters, and still be able to describe all meaningful details: all variants are completely defined by the initial hull form (in the usual B-spline surface description) plus a few parameters of the deformations. The designer then selects the deformation modes relevant for the case considered. A designer sets the location and size of the deformation box. Next, move a face, edge or corner point of that box by pulling. Pulling the front face forward caused a longitudinal extension of bulb; pulling the front top edge upward caused a bulb tilting; moving a corner point can produce other deformations. The deformations were shown instantly in the perspective window and in the waterlines, sections and buttocks plan. For higher-order boxes, there are also intermediate faces, edges and points that can be manipulated. An important property of the method was that a fair shape,

and a fair transition from the deformed to the unreformed part, was achieved. The designer applied the kind of deformation as wishes, and sets the maximum amount of deformation. Multiple boxes can be defined, for the same or different parts of the hull. In a session of an hour, the designer thus can define multi-parameter hull form families that are acceptable, satisfy geometric constraints and are hydro dynamically relevant for the case at hand. These properties are achieved by representing the box as a 3D B-spline of order 2, 3 or 4, *i.e.* any position inside the box is found from.

$$\vec{x}(\xi, \eta, \zeta) = \sum_{i=1}^I \sum_{j=1}^J \sum_{k=1}^K \vec{b}_{i,j,k} B_i^p(\xi) B_j^q(\eta) B_k^r(\zeta)$$

where x is the position vector as a function of three parameters ξ, η, ζ , $b_{i,j,k}$ are the box control points and B_i, B_j and B_k are the B-spline basis functions in the three directions. Suppose the hull form is described by the control points d_i , ($i = 1, \dots, N$) of the B-spline surface. Then to those control points are assigned, according to their position in the deformed box. Next the box is deformed by moving the box control point's $b_{i,j,k}$ to $b'_{i,j,k}$. This deformation is then applied to the surface control points d_i as well with the original. By moving control points instead of the hull shape itself, the hull remains smooth.

For this transformation type, first it is needed to create bspline volume (*i.e.* a box) that surrounds the geometry. For this box, the continuities can be further defined, which fixes some of the control vertices of the box. Finally you can choose from a set of operations that are applied to the geometry that is within the transformation box.

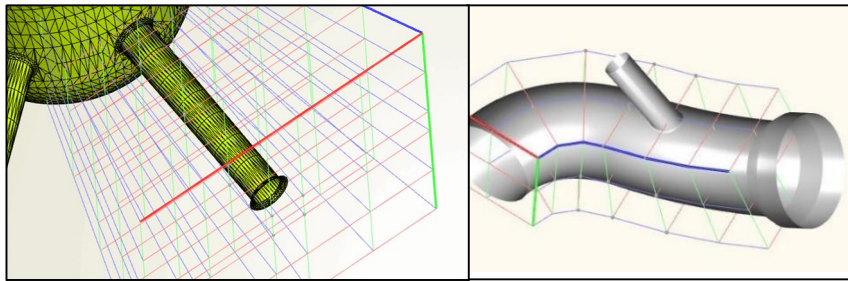


Fig. 3.1 Geometry deformed by free form deformation method [5]

3.5 Case Study

The study relies on a DTC container vessel. Duisburg Test Case (DTC) is a hull design of a modern 14000 TEU post-panama container carrier, developed at the University of Duisburg-Essen, Duisburg, Germany.



Fig.3.2 DTC hull 3D model

Table 3.1 Main dimension of DTC in design loading conditions

		Real Ship	Model Scale
Length between perpendiculars	L_{pp}	355 m	5.976 m
Waterline breadth	B_{wl}	51 m	0.859 m
Design draft amidships	T	14.5 m	0.244 m
Moulded depth	D	32.0 m	0.572 m
Block coefficient	C_b	0.661	0.661
Volume Displacement	V	173467.0 m ³	3.244 m ³

$V_1 = 22$ knots and $V_2=25$ knots was considered as the main condition for optimization process at the design draft of $T=14.5$ m. Different optimization approaches were used at the above two speeds. Each optimum model at the corresponding speed, the comparison of its hydrodynamic performance were made for different operation conditions.

3.6 Remodeling of Bow and Stern of DTC hull to Parametric Model

Since the idea of this research work was to minimize the resistance by refitting a bulbous bow and stern, the parametric model for this task was focused on the bulbous bow region and stern region only and maintained the section shape at the other area is fixed. Instead of changing the whole geometry into parametric, a partial parametric model was used. Such kind of parametric was that a baseline geometry definition which was transformed by means of various shift and scaling functions. To perform optimization the vessel, some parameters were selected to control the changes on the selected area of the geometry. The selection of parameters was based on an extended study of the influence of each variable regarding its optimization improvement i.e. the “capability” of each parameter on reducing the wave resistance and total resistance of the vessel.

DTC hull modelled was exported in STL format to CAESES as it was only needed to remodel bow and stern part of the vessel. As described above, free form deformation method was used to get partial parametric model in order to get different bulb shape by changing selected design parameters.

First b-spline box was created for bow transformation. This box determined the area in which the deformation was applied. B-spline box consist of 5 control points in each x, y, and z direction. So the box consist of total 125 control points to deform the geometry.

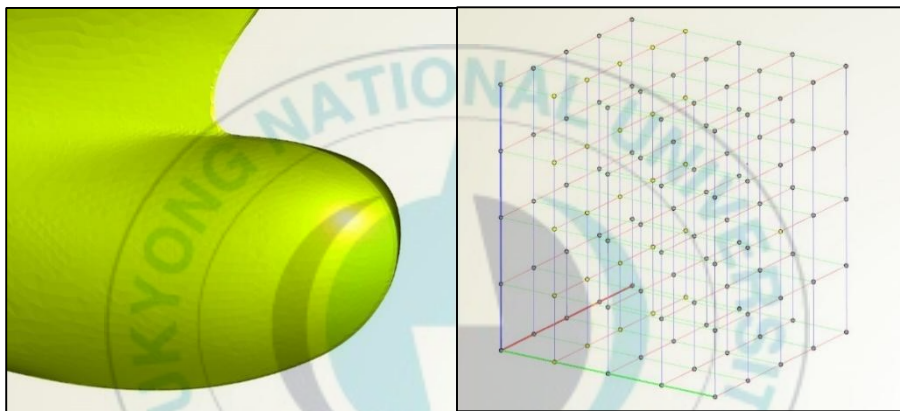


Fig. 3.3 B-spline control box and bulbous bow of the model

The procedure for stern deformation was also the same as the bow. B-spline box created around the stern and the parameter controlled the box to deform the transom height. The advantage of this deformation method was one parameter can control more than one control points. This helped in the optimization loop which can reduce the design parameters.

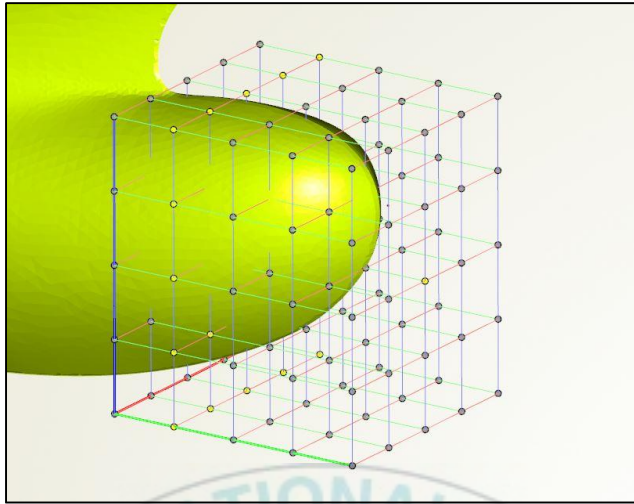


Fig. 3.4 Parametric modelling of bulbous bow using control B spline box

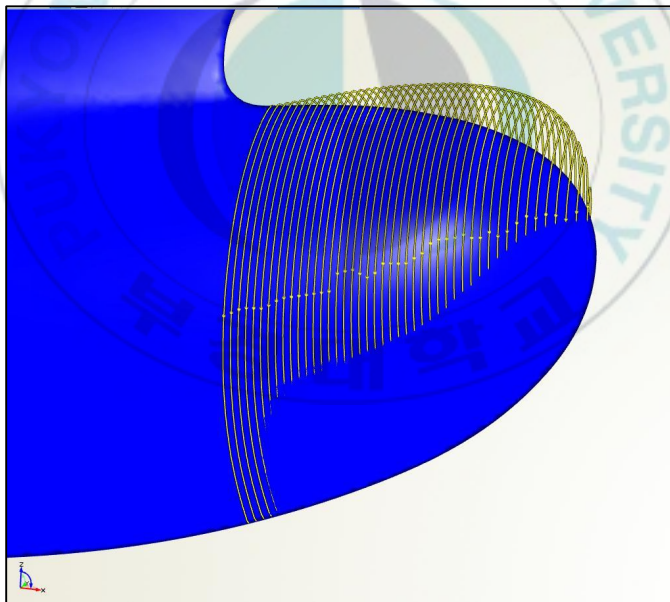


Fig. 3.5 Initial surface and new sections after free form deformation

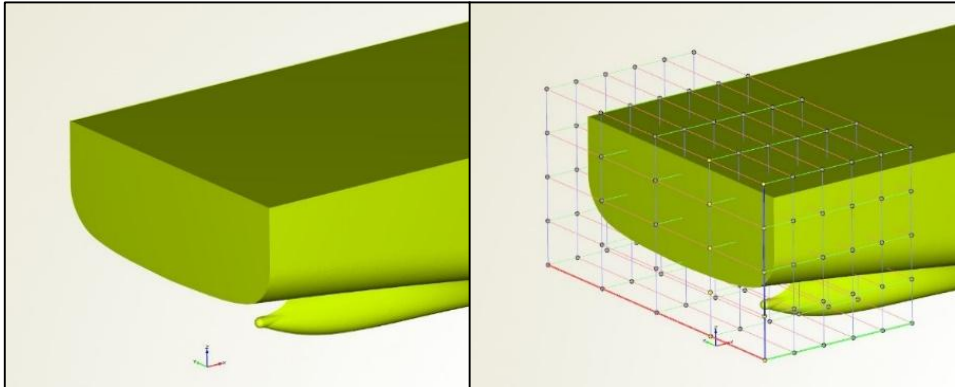


Fig. 3.6 Parametric modelling of stern using control B spline box

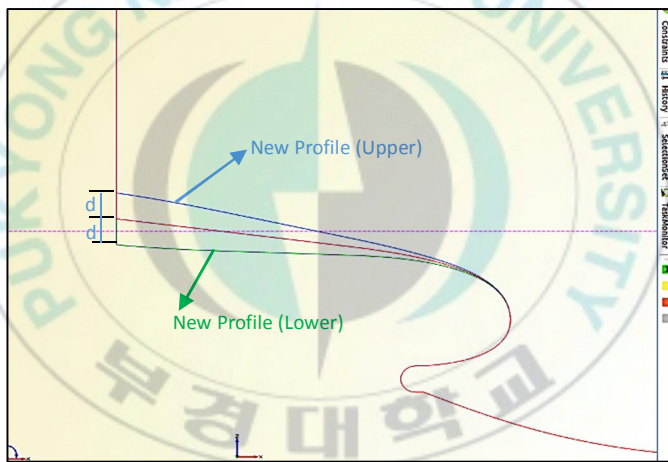


Fig. 3.7 Initial profile of stern and new profile after free form deformation

The detail set up and usage for free form deformation can be seen through CAESSES site [5].

3.7 Selection of Design Parameter

After generating the partial parametric model, there were 5 parameters controlling the bulbous bow shape variation in total. Some parameters had large effect on the changing of the bulb geometry and some only had little influence. Furthermore, the principal parameters that define the main dimension of the hull form cannot be changed. The number of design parameters should be as minimum as possible in order to be more efficient in the optimization process. The large number of design variables can lead to the very large amount of designs while combining all parameters. The design of experiments (DoE) study provides information to classify the design variables in order of influence to the resistance reduction. Therefore, it was necessary to define the important design variable parameters in order to save computational time and to be user-friendly for those who do not know the details of the parametric model. The variation scaled reference to the model scale of DTC hull.

- (a) **Bulb Length** – A shift of a longitudinal of the bulb sections allowed elongation or shortening of the bulbous bow. The variation ranged for the longitudinal position of bulb tip from base design was from -0.005 m to +0.005 m.
- (b) **Bulb Width** – This allowed for changes in width of the bulb. The variation range for the half width of the bulb from base design was from -0.0005 m to +0.0005 m to match the unaltered hull shape.
- (c) **Bulb Height**– A shift in the vertical section of the bulb allowed the bulbous bow tip to be lowered or raised with respect to the baseline bulb. The variation range of bulb tip elevation from the original base design was from -0.005m to +0.005m.

- (d) **Bulb Tangent Angle**– It was the inclination of the after part of the bulb that connects it to the hull. It ranges from -15 degree to 15 degree.
- (e) **Bulb Entrance Angle** – This parameter controlled the entrance angle of the waterline at the bow regarding the X-Y plane. Changing the angle of DWL at forward perpendicular at design waterlines, ranging from -15 degree to 15 degree (zero degree for base design).
- (f) **Transom Height**-This parameter defined the height of the transom .More transom height will lead to more underwater surface (more wetted surface area).This parameter ranged from -0.03 to 0.03m.

Table 3.2 Design variable and % difference to Original

Design Variable	Lower Limit	Upper Limit	Difference
Bulb Length(m)	-0.005	+0.005	3.0 %
Bulb Width(m)	-0.0005	+0.0005	2.5 %
Bulb Height(m)	-0.005	+0.005	2.5 %
Tangent angle(deg)	-15	+15	15 deg
Entrance angle(deg)	-15	+15	15 deg
Transom Height(m)	-0.03	+0.03	5 %

Chapter 4: Computational Fluid Dynamics (CFD)

Method

To be able to get ship hull's hydrodynamic performance optimization, CFD solvers involves as an important role to compute the flow fields at different operation conditions. The accuracy, computation time and reliability are mainly need to be considered while choosing CFD solver for the optimizing process. There are a lot of effective, reliable and fast commercial CFD tools for evaluating the numerical solution .In this work, open Source code OpenFOAM was used as a CFD solver. As it is an open Source, the user doesn't need to worry financial problem .OpenFOAM run in Ubuntu Operating System. The resistance was calculated using scaled models and the results were compared with the model Experimental result before optimization process.

4.1 OpenFOAM Theoretical Background

OpenFOAM (Open Source Field Operation and Manipulation) was an open source code using C++ language. Fig. 4.1 shows the workflow of OpenFOAM. In fluid dynamics, there are three physical laws that govern a fluid flow:

- (i) Conservation of Mass,
- (ii) Conservation of momentum (Newton's Second Law).
- (iii) Conservation of Energy

However, these equations cannot be solved analytically until now. One alternative is to solve them numerically using Computational Fluid Dynamics

(CFD). In real applications, fluids flow is turbulent and it can be modeled by RANS (Reynolds Averaged Navier Stokes) technique.

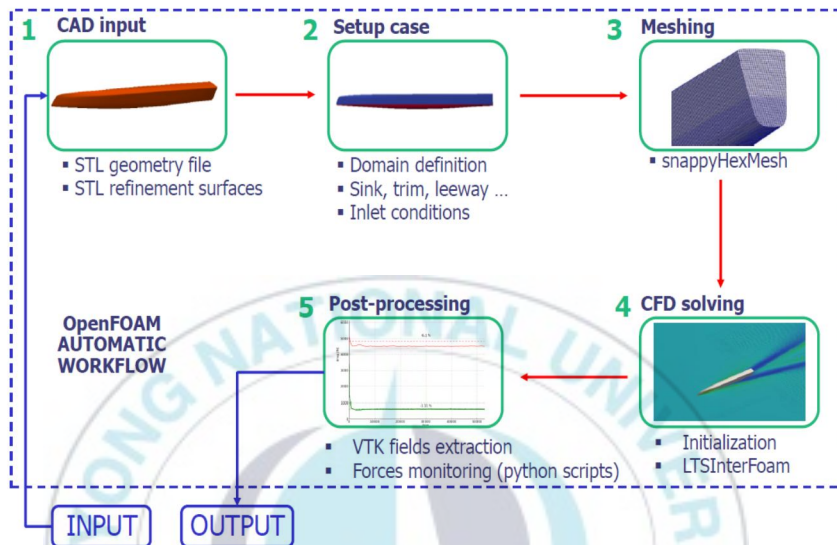


Fig. 4.1 CFD computation steps [14]

Free surface computation can be done in two methods, the interface tracking method and the front capturing methods. The Volume of Fluid (VOF) method is used the front capturing method for the free surface. Moreover, it is a two phase surface compression method that solves the Navier-Stokes equations and an additional advection transport equation for the volume fraction or scalar indicator function. The phase of the each cell can be described by alpha function. The alpha value 1 means that the whole cell is filled with water and 0 means the cell is filled with air, [12], [13].

4.2 Domain, Grids and Boundary Conditions

The computational domain was built as a rectangular block around the hull 2 times forward and 5 times of hull length at the backward as in Fig. 4.2 to avoid the effect of boundary. Fig.4.2 shows the boundary set up for the domain.

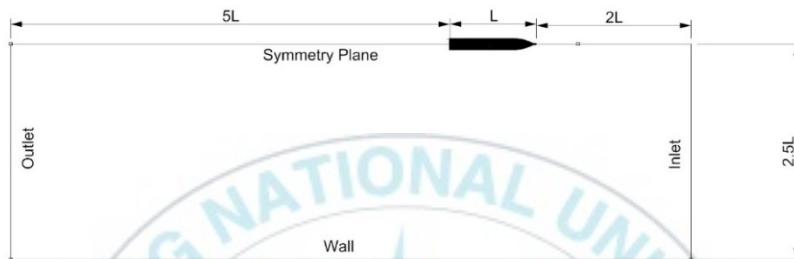


Fig 4.2 Domain grid and boundary conditions set up

4.3 Meshing

SnappyHexMesh (Built in meshing tool in OpenFOAM) can be used to create Mesh. SnappyHexMesh is a fully automatic, parallel, refinement based mesh generation app for OpenFOAM. The geometry type supports in OpenFOAM is Stereolithography (.stl) file .In constant folder, there is subfolder of triSurface and .stl file have to be exported here. For mesh region refinement TopoSetDict can be used to set the region to refine the mesh. In InterForm built-in folder Six toposet dictionary file are used to refine the desired region of domain.

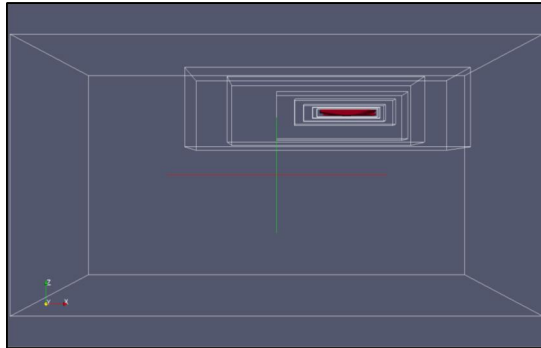


Fig. 4.3 Meshing (refinement) using SnappyHexMesh

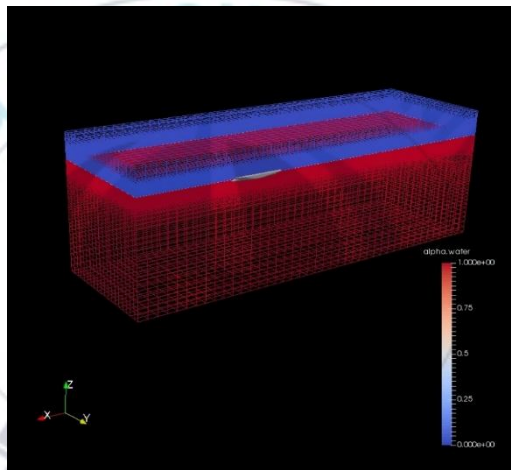


Fig. 4.4 Mesh domain filled with water (red) and air (blue)

4.4 Use of InterFoam Solver

In OpenFOAM package, there are different kinds of solvers that can be used for various sectors. For maritime related case, multi-phase solver like InterFOAM, InterDymFOAM and LTS interFoam can be used. The way to import geometry and meshing is already described above. Simulations parameters like start time, end time, deltaT, write control, etc. can be set in the controlDict dictionary file. In the folder “constant” parameters like viscosity,

gravity and the turbulence can be set. In transport properties dictionary, the fluids are set to be water and air. The turbulence model is set as k-omega SST model for this simulations. Since the resistance calculation is made using scale models and the speed is scaled using the Froude number.

$$Fr = \frac{V}{\sqrt{gL}}$$

where V is velocity, g is gravity and L is length, [14]. The simulation was run by Allrun script (can be seen in Appendix) .After running the simulation, the forces acting on the hull can be found in post processing file. To visualize the convergence of the simulations, Fig. 4.5 shows the force time history (3,000) seconds. Three thousand values of resistance were generated at 25 knots. OpenFOAM calculate the forces into two components acting in hull, namely viscous and pressure. Total resistance was obtained by adding pressure and viscous forces. Fig. 4.6 shows the flow pattern around the hull at 25 knots.

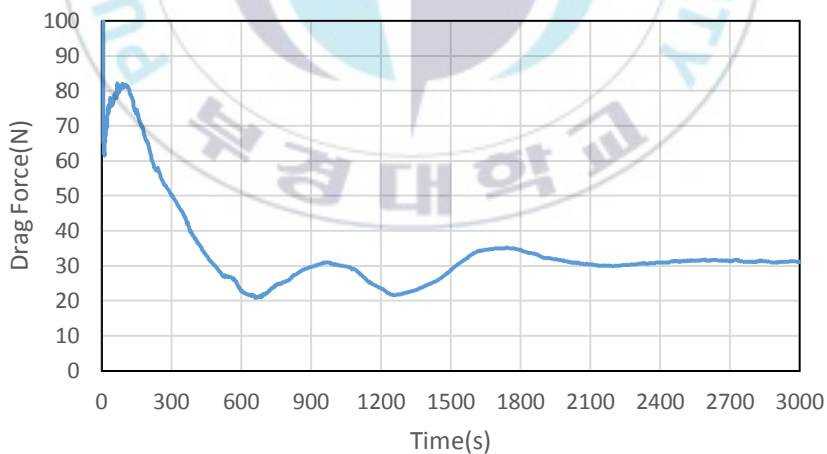


Fig .4.5 Convergence history of the DTC hull at 25 knots

4.5 Validation of OpenFOAM Results with Experimental Data

Resistance was measured at six forward speeds, corresponding to Froude numbers from 0.174 to 0.218 and full-scale advance speeds V_s from about 20.0 to 25.0 knots. The hull was ballasted at the design draft 14.5 m with zero trim. Tests were carried out at water kinematic viscosity = $1.09E-06 \text{ m}^2/\text{s}$ and density 998.8 kg/m^3 .

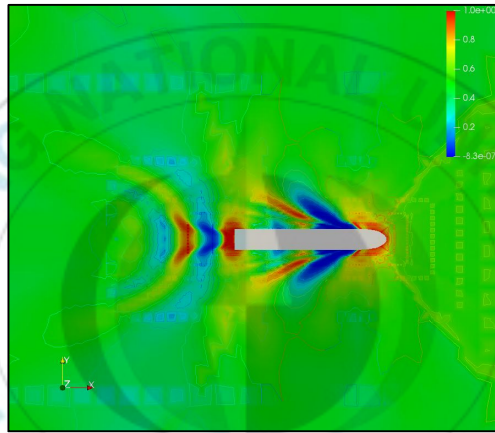


Fig. 4.6 Flow pattern around the DTC hull

Table 4.1 shows the experimental results referring to the model scale, including model speed V_m [m/s], Froude number [Fn], Reynolds number [Re], total resistance [R_m] and its non-dimensional coefficient [C_{tm}], frictional resistance [R_{fm}] and its non-dimensional coefficient [C_{fm}] and non-dimensional wave resistance coefficient [C_{wm}]. Their related equation are described below.

$$C_{tm} = \frac{R_{tm}}{0.5 \times \rho \times S \times V^2}$$

$$C_{fm} = \frac{0.075}{(\text{Log Re}_m - 2)^2}$$

$$C_{wm} = \frac{R_{wm}}{0.5 \times \rho \times S \times V^2}$$

Table 4.1 Results of resistance model tests

Vs (kn)	V _m (m/s)	F _n	Re _m x 10 ⁻⁶	Ct _m x 10 ³	Cf _m x 10 ³	C _{wm} x10 ⁴	Rt _m (N)	R _{wm} (N)
20	1.335	0.174	7.3198	3.6606	3.1695	1.9316	20.34	1.0733
21	1.401	0.183	7.6816	3.6049	3.1423	1.6714	22.06	1.0228
22	1.469	0.192	8.0545	3.5880	3.1160	1.7907	24.14	1.2048
23	1.535	0.200	8.4164	3.6019	3.0919	2.1935	26.46	1.6113
24	1.602	0.209	8.7837	3.6231	3.0689	2.6590	28.99	2.1276
25	1.668	0.218	9.1456	3.6695	3.0471	3.3594	31.83	2.9141

Table 4.2 Results and comparison of base model simulations in OpenFOAM

Vs (kn)	F _n	OpenFOAM Result			Exp	Diffe rence	% error
		R _{pressure}	R _{viscous}	R _{tm}			
20	0.174	1.4841	8.2203	19.41	20.34	0.93	4.57
21	0.183	1.5467	9.0918	21.28	22.06	0.78	3.54
22	0.192	1.6684	10.1731	23.68	24.14	0.46	1.91
23	0.200	2.2178	11.0284	26.49	26.46	0.03	0.11
24	0.209	2.5250	11.6501	28.35	28.99	0.64	2.21
25	0.218	2.4970	12.7535	31.61	31.83	0.22	0.39

The comparison of the numerical results were simulated by OpenFOAM and the experimental results performed by HSVA were described along with the results obtained from OpenFOAM Solver in Table 4.2. It can be seen that the numerical simulation was done for six different forward speeds and its curve shows the same curvature as experimental data as in Fig. 4.7. Since the results obtained from the OpenFOAM have only little difference percent compared to the experiment, it can be proved that OpenFOAM can be used as reliable solver for CFD calculations in this thesis. Next section will be continued with optimization process.

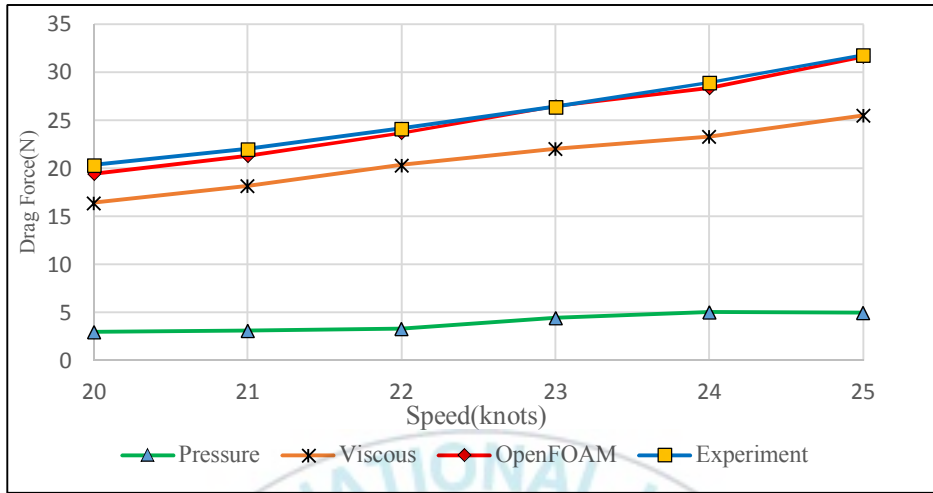
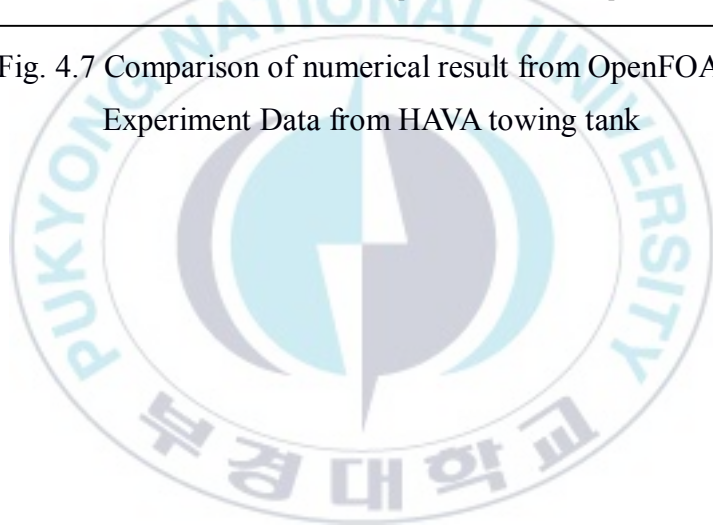


Fig. 4.7 Comparison of numerical result from OpenFOAM and Experiment Data from HAVA towing tank



Chapter 5: Optimization Process in Calm Water Condition

Ship hull design is a complex task. Optimization plays an important role in order to get the best design. However, a lot of computational time is needed and costly. Nowadays, as the technology develops, computer are more powerful and hundreds of designs can be simulated and optimized in a short time. In this thesis, optimization process in calm water condition at two speed, will be performed with different methods. The objective functions is to minimize total resistance at the design draft of 14.5m at two operating speeds of 22 knots and 25 knots. The Surrogate model (also known as meta-model or response surface) is used, to approximate an original high fidelity model. The surrogate acts as data fit to the observations so that new results can be predicted without recurring to expensive simulations:

5.1 Design of Experiments

In this thesis, the optimization processes was applied to perform a study of the design space. Usually the Design of Experiments (DoE) was driven by a random or quasi-random process (SOBOL in CAESES) and it had a big importance as well to drives the optimization process to get the optimum. Designers can determine simultaneously the individual and interactive effects of many factors that could affect the output results of the design with DOE as shown in Fig. 5.1. According to the results from design of experiment, the best design can be selected and the optimization method is performed based on it.

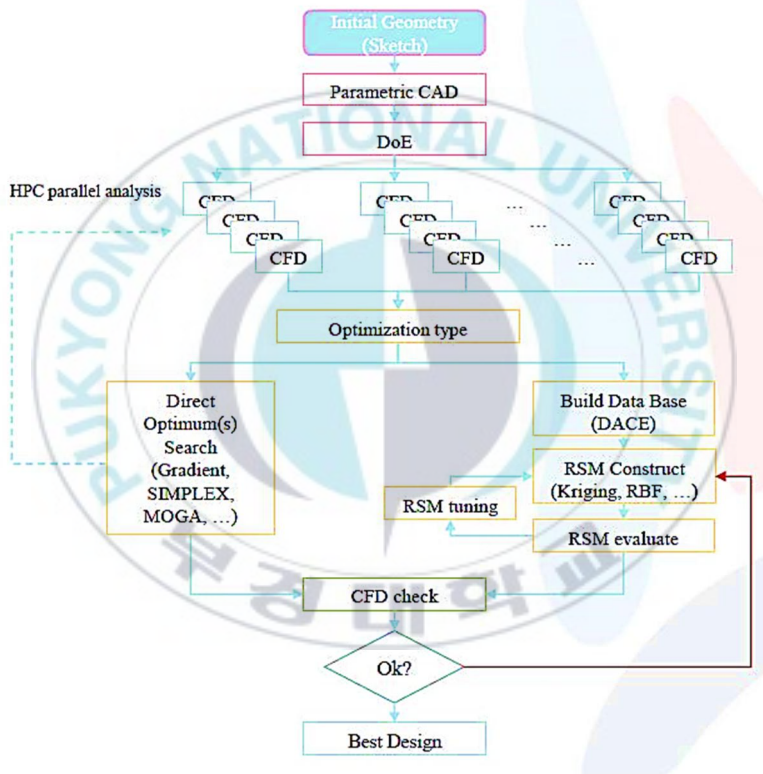
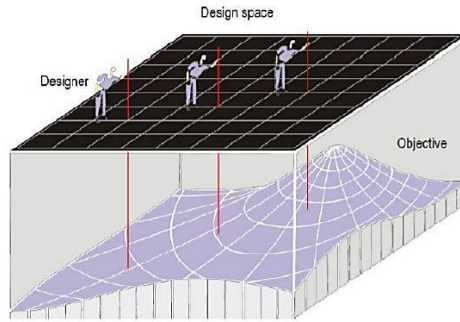


Fig.5.1 Surrogate based optimization process [15]

5.2 Software Connection

CAESES[®] is an integration platform that can launch and control CFD runs or any other simulation processes. CAESES[®] itself has no simulation solver such as CFD tools to create a closed loop. Moreover, it can be used as Post Processing GUI (graphical user interface) for any external software. Basically, any external tool that can be run in batch mode can be coupled in just a few minutes. In here, CFD solver is coupled but any other CAE or preliminary design tool coupling can be possible – the entire data exchange and management is controlled by CAESES[®].

The performance function within the CAESES are

- Export of geometry using common CAD formats (e.g. IGES, STEP, ACIS, various STL formats) automatically to black box solver.
- Easy definition of geometry using Feature Definition function.
- Post-Processing visualization capability (GUI)
- Result value from the CFD can extract easily.
- Coupling of multiple external tools and setting up sequential process chains, e.g. meshing > simulation 1 > simulation 2 > ... > post-processing.

Firstly, the parametric geometry must be watertight .stl file in order to run in OpenFOAM. The software connector is the widget where external tools can be plugged-in. The figure shows the software connector interface and is divided as four parts like Input Geometry, Input files ,Result Values and Result Files. The parametric .stl file was inserted in input geometry part .The OpenFOAM executable files were put in input files part. OpenFOAM “Allrun” script file needed to modify in order to run in the CAESES. The Allrun file script is shown in Appendix. For post processing of the result, it

was needed to create the “case. Foam “file by adding the following command into the Allrun script. Results files and values were needed which will be inserted in the Results Files and Results Values window of the software connector. In order to get these, it was needed trigger a first run – either with CAESES or externally. In here CAESES ® was used as a trigger run .Next the computation “Runner” was set up. A new folder was created, with the name of the current project file (*.fdb). In this folder, all results of the run can be found. In order to assess the optimization, it was needed to have result files which provide for resistance of the hull. These values can be extracted from any text files, but usually from *.csv or *.dat file formats. Since CAESES ® needed to know where the desired values are located in each design directory, output files from the CFD calculation were referenced in the Result Files window of the connector. Then coupling of OpenFOAM solver and CAESES was completely set up.

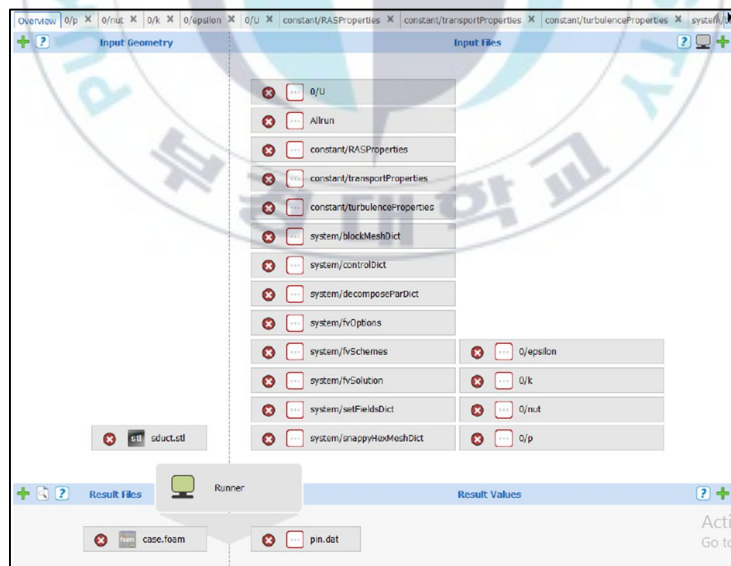


Fig. 5.2 Software connector interface

5.3 Single Objective Optimization

5.3.1 Case 1(Bow) - minimize total resistance at V=25 knots at design draft of 14.5m

The first case was single objective optimization process and Local Optimization Efficient method in Dakota interface was used starting from the initial design selection from Design of Experiments (SOBOL). This method was surrogate-based local optimization. For the initial surrogate model, data was taken from Design of Experiments, [15].

As this was an integrated optimization of bow and stern, the bow was optimized first. Next the optimized bow was chosen as a base model for the stern optimization part. The optimization process were performed for 50 designs in which 20 designs were chosen as the samples for initial surrogate model. The process took 8 days approximately 1 week running in a computer with the processor of Core™ i7-2760QM CPU @ 2.40 GHz, RAM 16GB. Detail result output can be seen in the Appendix A. Fig.5.3 presents the results for the optimization process and table 5.1 shows the difference in total resistance (4.8327%) relative to the base model for 25 knots.

Table 5.1 Comparison of base design and optimized bow at 25 knots

Speed (kn)	Base Design	Optimized Design	Difference	%reduction
25	31.6153	30.0874	1.5279	4.8327

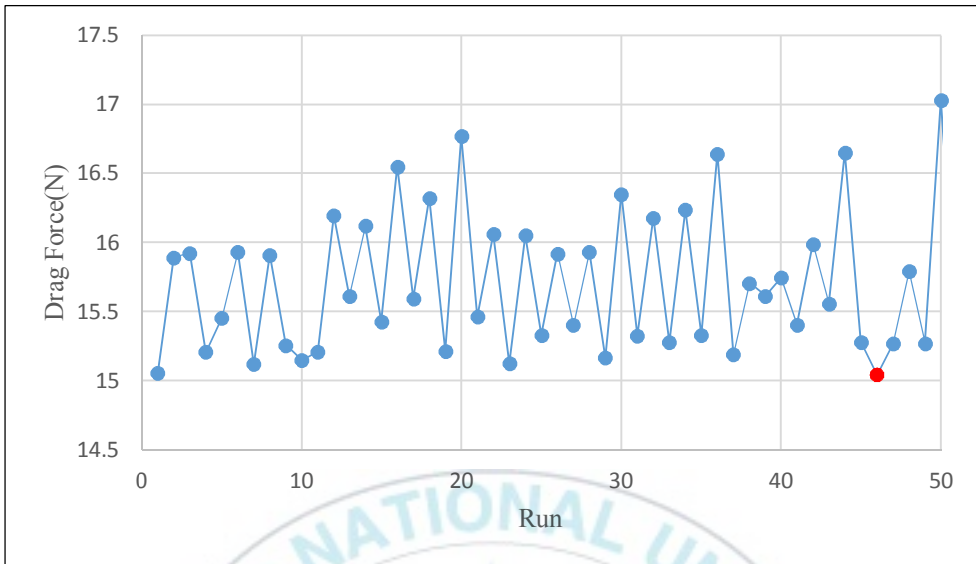


Fig. 5.3 Single objective optimization of bow at 25 knots

5.3.2 Case 1(Stern) - minimize total resistance at V=25 knots at design draft of 14.5m

At the speed of 25 knots, the bow was optimized first and the stern shape was optimized next to reduce the resistance more with Dakota/ Local optimization efficient strategy. Fig.5.4 presents the results for the optimization process and table 5.2 shows the difference in total resistance (7.2917%) relative to the base model for 25 knots.

Table 5.2 Comparison of base design and optimized design of stern at 25 knots

Speed(kn)	Base Design	Optimized Design	Difference	%reduction
25	31.6153	29.3100	2.3053	7.2917

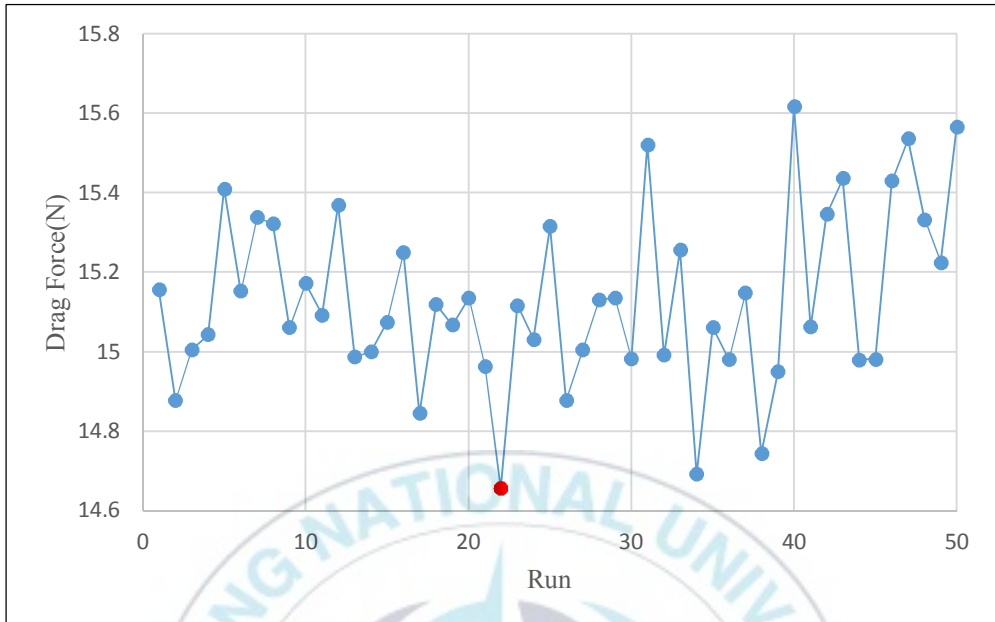


Fig. 5.4 Single objective optimization of stern at 25 knots

5.3.3 Case 2 (Bow) - minimize total resistance at V=22 knots at design draft of 14.5m

The same procedure was applied to optimize the model at 22 knots. Fig.5.5 presents the results for the optimization process together with the designs obtained on the DoE study, the difference in total resistance 4.6481% relative to the base model for 22 knots.

Table 5.3 Comparison of base design and optimized design of bow at 22 knots

Speed(kn)	Base Design	Optimized Design	Difference	%reduction
22	23.6442	22.5452	1.099	4.6481

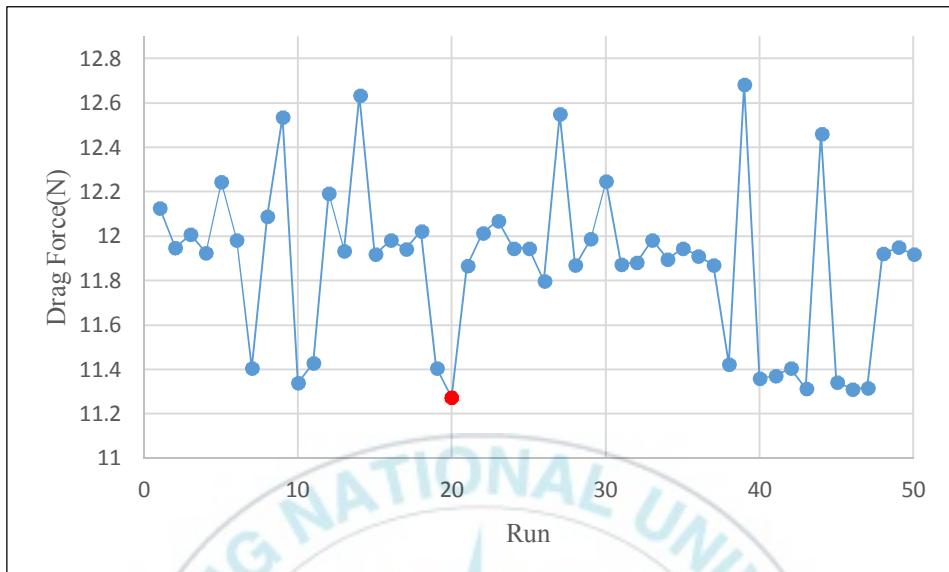


Fig. 5.5 Single Objective Optimization of bow at 22 knots

5.3.4 Case 2 (Stern) - minimize total resistance at V=22 knots at design draft of 14.5m

The same procedure followed as described above. Here, the base line hull was from the optimized bow at 22 knots. Fig. 5.6 shows the result of optimization of stern after 22 knots. In comparison with based model, the optimal model for V=22 knots had a reduction of 6.4904% in total resistance of the ship.

Table 5.4 Comparison of base design and optimized design of stern at 22 knots

Speed (kn)	Base Design	Optimized Design	Difference	%reduction
22	23.6442	22.1096	1.5346	6.4904

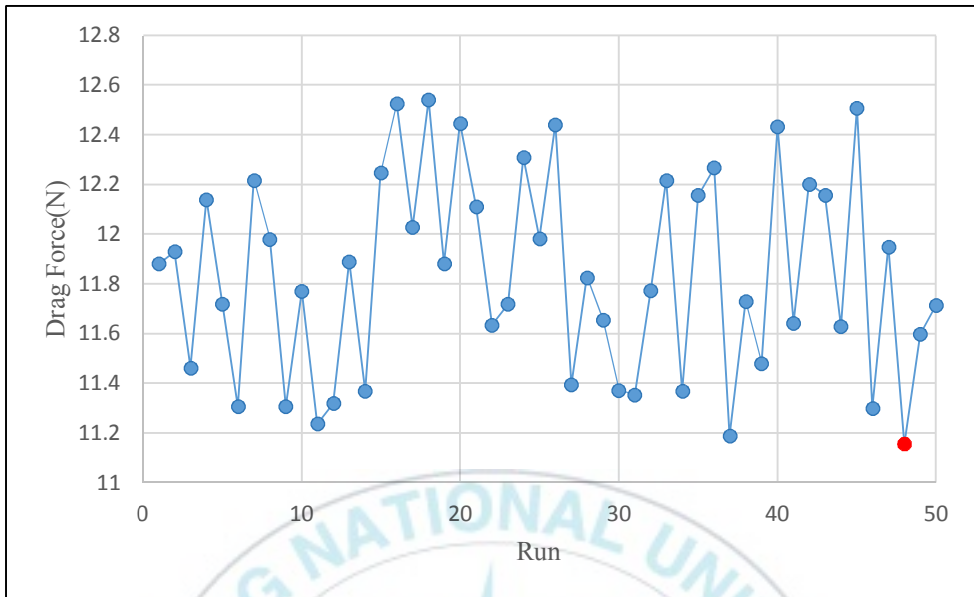


Fig. 5.6 Single objective optimization of stern at 22 knots

5.4 Multi-objective Optimization

In reality, most of the optimization problems involve more than one objective to be optimized. From the maritime point of view, most of the ships are needed to operate at different conditions and speeds optimized design and designing one-speed, one-condition optimization is not efficient. In order to solve this kind of problem, CAESES which can generate a large number of hull forms over a range of conditions and speeds is very efficient tool while checking that any constraints are not broken. A hull form which is fine tuned to operate at the exact operational profile given by the ship owner can be obtained as a result. The CFD solver OpenFOAM is running outside and result is put in CAESES interface and DAKOTA is produce variable and letting CAESES take care of hull changes and ranking of designs. For multi-objective optimization process in CAESES with Genetic algorithms are used.

Genetic Algorithms can be used to solve this type of problems. The GA concept was developed by Holland and his colleagues in the 1960s and 1970s. GA are inspired by the evolutionist theory explaining the origin of species. In nature, the weak and unfit species are removed by natural selection. The strong ones have greater opportunity to pass their genes to future generations via reproduction. In the long run, species carrying the correct combination in their genes become dominant in their population. Unsuccessful changes are eliminated by natural selection. GA operate with a collection of chromosomes, called a population. The population is normally randomly initialized. As the search evolves, the population includes fitter and fitter solutions, and eventually it converges, meaning that it is dominated by a single solution. Holland also presented a proof of convergence (the schema theorem) to the global optimum where chromosomes are binary vectors. GA use two operators to generate new solutions from existing ones: crossover and mutation. The crossover operator is the most important operator of GA. In crossover, generally two chromosomes, called parents are combined together to form new chromosomes, called offspring. The parents are selected among existing chromosomes in the population with preference towards fitness so that offspring is expected to inherit good genes which make the parents fitter. By iteratively applying the crossover operator, genes of good chromosomes are expected to appear more frequently in the population, eventually leading to convergence to an overall good solution. The mutation operator introduces random changes into characteristics of chromosomes. Mutation is generally applied at the gene level. In typical GA implementations, the mutation rate (probability of changing the properties of a gene) is very small and depends on the length of the chromosome. Therefore, the new chromosome produced by mutation will not be very different from the original one. Mutation plays a

critical role in GA. As discussed earlier, crossover leads the population to converge by making the chromosomes in the population alike. Mutation reintroduces genetic diversity back into the population and assists the search escape from local optima. Reproduction involves selection of chromosomes for the next generation. In the most general case, the fitness of an individual determines the probability of its survival for the next generation. There are different selection procedures in GA depending on how the fitness values are used [16],[17],[18].[19].

5.4.1 Case 3 (Bow) - minimize total resistance at V=25 knots and V=22 knots (Multi-Objective) at 14.5 m

In this case, the bulbous bow was optimized considering two operating speed of 25 knots and 22 knots. The multi-optimization process using genetic algorithm was performed for 50 designs. The results for the multi-objective optimization by means of genetic algorithms can be seen in Fig. 5.7. The total resistance related to base model is approximately 5.4056% reduction at 25 knots and 4.4641% reduction at 22 knots.

Table 5.5 Comparison of base design and optimized design of bow at two speed (multi-objective)

Speed (kn)	Base Design	Optimized Design	Difference	%reduction
25	31.6153	29.9063	1.7090	5.4056
22	23.6442	22.5887	1.0555	4.4641

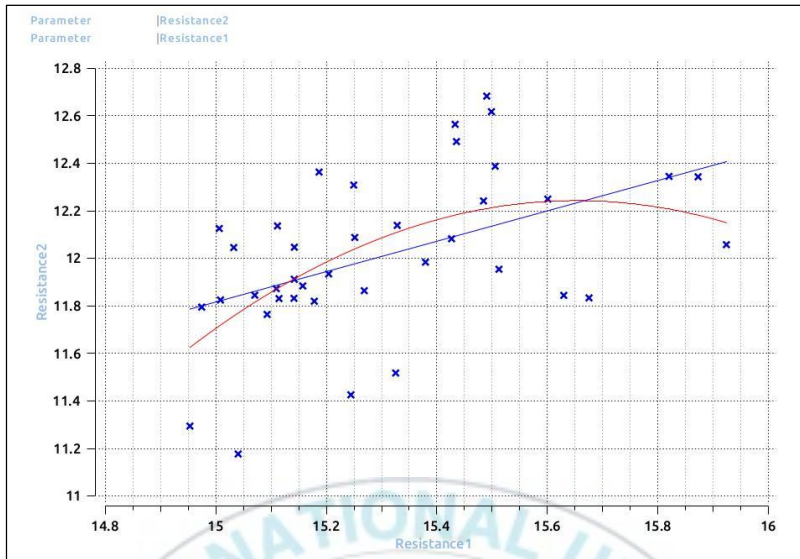


Fig. 5.7 Multi-Objective optimization of bow (MOGA)

5.4.2 Case 3 (Stern) - minimize total resistance at V=25 knots and V=22 knots (Multi-Objective) at 14.5 m

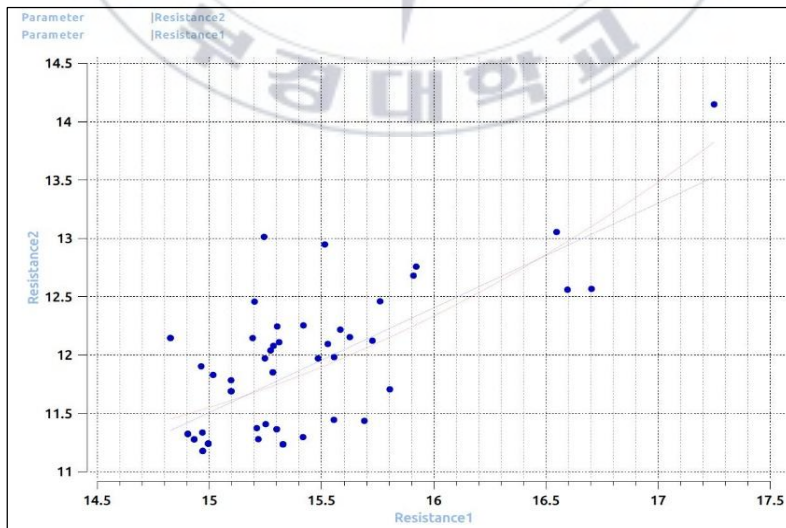


Fig. 5.8 Multi-Objective optimization of stern (MOGA)

As like in single objective, the optimized bow obtained for multi-objective was used for stern optimization. The results can be seen in Fig. 5.8 Here, there were there design that give optimum. So it was needed to decide which one can give the best for optimum. The decision making for choosing optimum was described in Chapter 6. The percent reduction of each design can be seen in Table 5.6.

Table 5.6 Comparison of base design and optimized design of stern at two speed (multi-objective)

Design 5				
Speed (kn)	Base Design	Optimized Design	Difference	%reduction
25	31.6153	29.8643	1.7510	5.5225
22	23.6442	22.5303	1.1097	4.6942
Design 18				
25	31.6153	29.8074	1.8079	5.7026
22	23.6442	22.6493	0.9949	4.1906
Design 36				
25	31.6153	29.9403	1.6750	5.2819
22	23.6442	22.3571	1.2871	5.4267

Chapter 6: Results and Analysis

The number of CFD runs to perform the optimization for each method is shown in table 6.1 for the speed of $V_1=25$ knots and $V_2=18$ knots at the design draft of $T=14.5\text{m}$. The chosen optimum design for each case is also described in the table.

Table 6.1 Number of CFD run for each case

		CFD Run (DOE+Opt)		Optimum Design
		BOW	STERN	
Single Objective	DOE+Surrogate based local optimization	20+50	20+50	SO-V25
		20+50	20+50	SO-V22
Multi- Objective	Dakota MOGA(surrogate based global optimization)	20+50	20+50	MO-Des5
				MO-Des18
				MO-Des36

6.1 Analysis of Optimal Models at Different Operation Conditions

From the result table, optimal model was obtained for each case. But in reality it was needed to choose one optimal among these. Since the optimization process was performed for $V_1 = 25$ knots and $V_2 = 22$ knots at the design draft of $T = 14.5\text{m}$, the selected optimal models from each

optimization process were analyzed also for different operation conditions as shown below. After that it is possible to choose optimum model which performance is better. Table 6.3 shows the result of each optimum model at different operation conditions and Table 6.4 in terms of different percent compared to base model.

Table 6.2 Comparison of base design and optimized design for each case

Design	Speed (kn)	Base Model Rt	Optimum Model Rt	% Reduction
SO-V25	25	31.6153	29.3113	7.2917
	22	23.6442	22.8619	3.3087
SO-V22	25	31.6153	30.5408	3.3986
	22	23.6442	22.1096	6.4904
MO-Des 5	25	31.6153	29.8643	5.5225
	22	23.6442	22.5303	4.6942
MO-Des18	25	31.6153	29.8074	5.7026
	22	23.6442	22.6493	4.1906
MO-Des 36	25	31.6153	29.9403	5.2819
	22	23.6442	22.3571	5.4267

Slow Speed Scenario:

OC1: V= 15 knots, T=14.5 m

OC2: V= 18 knots, T=14.5 m

High Speed Scenario:

OC3: V= 22 knots, T=14.5 m

OC4: V= 25 knots, T=14.5 m

Table 6.3 Total resistance (N) for selected optimal models at different operation condition

	BM	SO V25	SO V22	MO		
				Des5	Des 18	Des 36
OC1	11.6699	11.8614	11.8065	11.5750	11.6394	11.5834
OC2	15.9878	16.2375	16.1610	15.9532	16.4940	16.0647
OC3	23.6442	22.8619	22.1096	22.5303	22.6493	22.3571
OC4	31.6153	29.3113	30.5408	29.8643	29.8074	29.9404

Table 6.4 Total resistance % difference for selected optimal models at different operation condition

	SO V25	SO V22	MO	MO	MO
			Des5	Des 18	Des 36
OC1	1.6406 %	1.1699%	-0.8138 %	-0.2617 %	-0.7705 %
OC2	1.5615 %	1.0827 %	-0.2168 %	3.1653%	0.4802 %
OC3	-3.3087%	-6.4906%	-4.6942%	-4.1906%	-5.4219%
OC4	-7.2877 %	-3.3986 %	-5.5225%	-5.7026%	-5.2819%

6.2 Optimal Model Selected from the Optimization in Calm Water

After considering all the performance of the designs obtained with single objective and multi-objective optimization processes, the design MO des 5 was selected as final optimal model. The reason why choose this design was it had not only reducing resistance at target speed but also can maintain the resistance at other speed.

This model had the improvement in total calm water resistance of 4.6942% and 5.5225% reduction for 22 knots and 25 knots respectively at the design draft $T=14.5\text{m}$. This model also had the improvements in different operation conditions. Fig 6.1 shows the comparison of optimal model at different speed with base model.



Fig. 6.1 Comparison of resistance of base model and final optimum for different speed

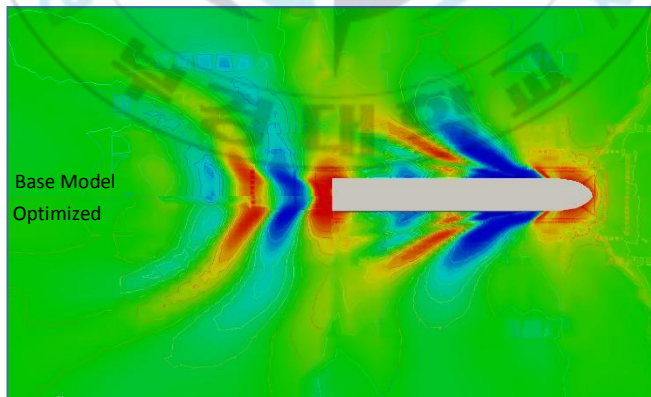


Fig. 6.2 Comparison of wave contour of base model and final optimum model

The wave profile generated by the vessel can be seen in Fig. 6.3 .The differences in the wave pattern can be seen in the bow and stern part .The optimum one has lower wave height at bow and stern compared to base model in Fig. 6.3. The optimized bulbous bow length, width and height differ only a few percent to original and the bulb tip a bit lower and the entrance angle a bit narrower than original. For stern, the transom underwater part was reduced around 4% than original.

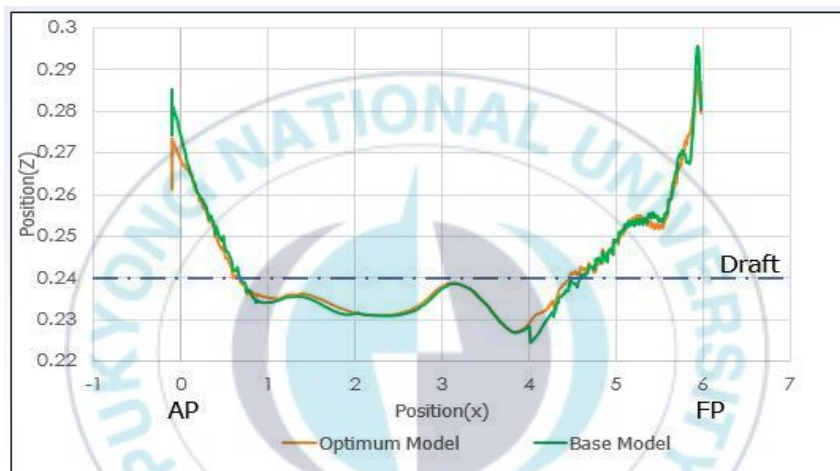


Fig. 6.3 Comparison of wave profile of base model and final optimum model

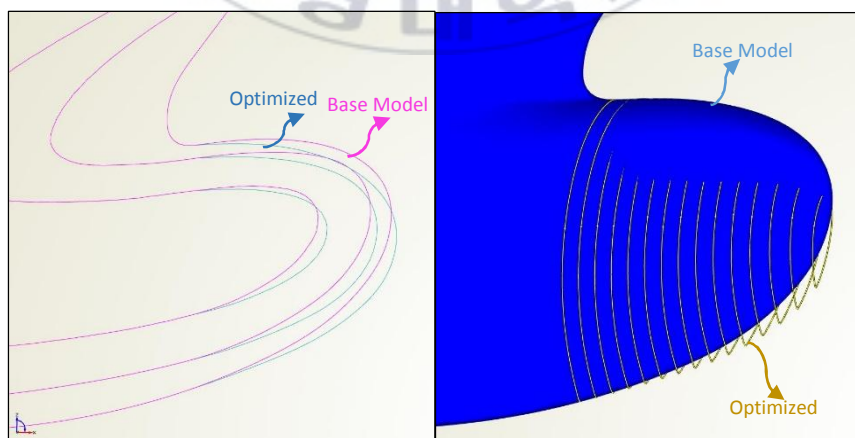


Fig. 6.4 Comparison of base model and final optimum bow model

Table 6.5 Geometry Variation trend of optimized bulbous bow

Design	Design Variable				
	Bulb Length	Bulb Width	Bulb Height	Bulb Tangent	Entrance Angle
Base Model	0.18 m	0.1 m	0.12 m	22.36 deg	90.33 deg
Optimized	0.1791 m	0.1002 m	0.1188 m	12.36 deg	86.67 deg
% Variation	0.5 % Shorter	0.158% narrower	1.058% lower	-10.0 deg	-3.66 deg

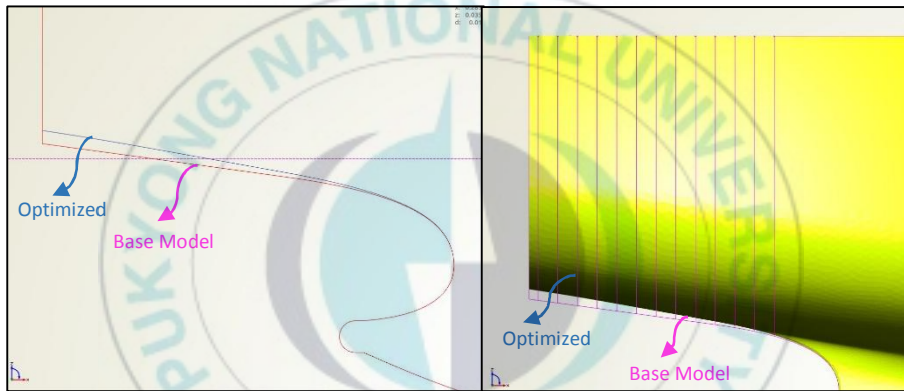


Fig. 6.5 Comparison of base model and final optimum stern model

Table 6.6 Geometry variation trend of optimized stern

Design	Design Variable	
	Transom Height (d)	% Variation
Base Model	0.315 m	-
Optimized	0.302 m	4% upward

Chapter 7: Summary, Conclusion and Future Works

7.1 Summary

In summary, the ship hull form was optimized in calm water condition in order to minimize the total resistance. In this thesis, geometry deformation method for modifying the parametric model of the initial model (Free Form Deformation) was described. Popular OpenSource CFD code OpenFOAM is used, followed by the validation of its results with the experimental data from HSVA towing tank.

The coupling of the CFD solver to the optimization algorithms in the framework of CAESES was done and shows the procedure of the automatic process of optimizing. In this thesis, the use of OpenFOAM solver coupling with CAESES / Dakota interface for optimization was introduced. To achieve optimum design, the study of DOEs in the design space was done first, followed by the single objective optimization for different speeds with Dakota. Not only single objective optimization for each speed but also the multi-objective optimization process was performed for both speed conditions at fixed draft.

In the stage of optimization in calm water condition, the different optimum designs for two speeds were then checked with initial model. Since the optimization was done for two speeds with fixed draft, the different optimal models was analyzed for different operation scenario and compared with initial model's performance.

7.2 Conclusion

Several conclusions can be made based the optimization techniques used in this thesis and the analysis of CFD code in order to get the reliable results

of the simulations. For achieving the good and feasible behavior in the optimization, the CFD solver should be used and OpenFOAM was the best fit for this process as it can be easily get as an OpenSource.

The single objective method gives to a very good improvement for the condition set as objective. The multi-objective optimization by means of genetic algorithm, MOGA, cannot give the best one .As in the nature, optimizing both the objective will be difficult to achieve.

The final optimal models obtained from optimization approaches gave the greater improvement when compared to the initial model. As conclusion, the proper selection of the optimization method for each case of study proves to be a key factor in order to achieve good results.

7.3 Future Works

For the optimization processes, it is important to have a good initial design that can be obtained via DoE (e.g. SOBOL method). It can be said that the optimization approaches in this work scope are not the complete task for the early design stage. This work was performed only for the optimization of bulbous bow and stern in calm water condition. Actually the whole under water hull have effect on reducing resistance. Since the purpose of this thesis is to get the optimal design by changing only fore and aft parts which has the better performance in calm water. Instead of OpenFOAM solver, faster potential flow code, DNV GL, Wavis can also be used. This process can also be test with Commercial CFD solver like Ansys, Star CCM+ to validate the result. The results obtained from overall analysis in this thesis are quite helpful and reliable for further detail analysis. In the future, the author will study more not only for resistance but also for seakeeping (resistance in waves).

References

- [1] Feng, B.W., Liu, Z.Y., Zhan C.S., Chang, H. and Cheng, X., 2008. “Automatic optimization techniques of ship hull based on CFD”. *Conference Proceedings Ship Hydrodynamics*, 26-29 November 2009
- [2] Chen, P.F., Huang, C.H., Fang, H.C. and Chou, J.H., 2006. “An inverse design approach in determining the optimal shape of bulbous bow with experimental verification”. *Journal of Ship Research*, 50(1), pp.1-14.
- [3] Harries S, February 2015, “Practical Shape Optimization Using CFD”, FRIENDSHIP SYSTEMS.
- [4] Dakota Version 6.1, User Manual, Chapter 14, Advanced Methods
- [5] CAESES4.1.2, Tutorials, “www.caeses.com”.
- [6] Zhang Ping, Zhu De-xiang and Leng Wen-hao, 2008, “Parametric Approach to Design of Hull Forms” ScienceDirect Journal of Hydrodynamics, 20(6), 804-810.
- [7] Abt, C.; Bade, S.D.; Birk, L.; Harries, S., September 2001, “Parametric Hull Form Design”.
- [10] Han, S.H., Lee, Y.S. and Choi, Y.B., 2012. “Hydrodynamic hull form optimization using parametric models.” *Journal of Marine Science and Technology*, 17, pp.1-17.
- [11] Harries, S., Abt, C. and Heimann, J., 2003. “From redesign to optimal hull line by means of parametric modeling.” *2nd International Conference on Computer Applications and Information Technology in the Maritime Industries (COMPIT 2003)*, Hamburg, Germany, May 2003.
- [12] Jacquin, E., Derbanne, Q., bellèvre, D., Cordier, S. and Alessandrini, B., 2004. “Hull form optimization using a free surface RANSE solver”

25th *Symposium on Naval Hydrodynamics*. Newfoundland, Canada, 8-13 August 2004.

- [13] Giovanni Bailardi*, Joel Guerrero, Damiano Natali “Fluid-Dynamic Design and Optimization of Sailing Yachts” using a complete Open Source Framework Authors:
- [14] Lilit Axnera,b, Jing Gong,a,b,* , Alessandro Chiarinic, Luigi Mascellaro “Hull resistance simulations for an innovative hull using OpenFOAM”
- [15] Tin Yadanar Tun , “Ship Hull Optimization in calm water and moderate sea states”, University of Rostock.
- [16] Dejhalla, R., Mrsa, Z. and Vukokic, S., 2002. “A genetic algorithm approach to the problem of minimum ship wave resistance”.*Marine Technology*, 39(3), pp.187-195.
- [17] Gregory J. Grigoropoulos and Dimitris S. Chalkias, 2009, “Hull-form optimization in calm and rough water”. *Computer-Aided Design*, 42 (2010), 977-984.
- [18] H. Bagheri, H. Ghassemi, 2014. “Genetic Algorithm Applied To Optimization of the Ship Hull Form With Respect to Seakeeping Performance”. *Transactions of Famena* Xxxviii-3.
- [19] Shahid Mahmood and Debo Huang, 2012, “Computational Fluid Dynamics Based Bulbous Bow Optimization Using a Genetic Algorithm” *Multihull Ship Technology*, Key Laboratory of Fundamental Science for National Defense, Harbin Engineering University, Harbin 150001, China

선형 자동 생성법과 다목적 최적화 기법을 이용한 선형 최적화

메이투저

부경대학교 조선해양시스템공학과

국문 요약

최근 국제적으로 친환경에 대한 관심이 증가하고 있고, 조선분야에서는 저항을 감소시킬 수 있는 최적선형 설계를 하는 것이 추세이다. 본 논문은 최적 설계에 대한 연구로 전체 저항을 최소화하기 위해 Calm Water 조건에서 최적화를 수행하였다. CFD 코드로 OpenFOAM을 사용하였으며, 먼저 CFD 결과와 실험 데이터를 비교하여 CFD의 적용가능성을 확인하였다. 적용 선형으로는 DTC를 사용하였으며, 선형을 수정하기 위해서 Free Form Deformation 방법을 사용했고, 최적화를 위해 CAESES / Dakota 인터페이스와 OpenFOAM 솔버 coupling을 소개하고, CAESES 프레임 워크에서 최적화 알고리즘과 CFD 솔버의 결합을 수행하여 최적화 과정을 자동으로 실행하였다. Dakota optimizer를 이용해서 Single Objective 최적화와 Multi-Objective(다목적 최적화) 프로세스도 수행하였다. Single Objective 방법은 객관적으로 설정된 조건에 대해 매우 좋은 결과를 제공하고, 유전자 알고리즘, MOGA에 의한 다목적 최적화는 최상의 것을 제공하기 어렵고 두 목적을 만족시키는 결과를 준다. 각각 선택된 최적모델을 다른 작동 조건에 대해서도 분석해서 최종 최적선형으로 선택하였다. 결론적으로, 최적화 접근법에서 얻은 최종 최적 모델은 초기 모델과 비교했을 때 저항이 더 낮은 것으로 나타났다.

키워드 : 선형 최적화, CFD, 유전자 알고리즘, 다목적 최적화

Acknowledgements

Firstly, I would like to express my special thanks to my advisor Professor Dong-Joon Kim of the Department of Naval Architecture and Marine Systems Engineering at Pukyong National University. He taught me what I don't know, explain me patiently and give good suggestions and plenty of support to me. Because of him, I can finally finish this thesis for my master degree. Without his support and encouragement, I cannot be able to finish this work.

I would like to thank all the other professors in our department for giving such a great lectures and knowledge related to Naval Architecture. The class are very interesting and it will be great help in my future career. I also would like to thank my seniors Yeon-Hee Song, Seung-Woo Shin and lab members Aldias Bahatmatka, Samuel, Zhang Yong Xing and Thandar Aung for supporting and treating like a family member and give helpful suggestions and discussions throughout this research. Because of them, I enjoyed student life in Korea.

I am also thankful to NIIED (National Institute for International Education of Korea) for the scholarship fund. I greatly appreciate their support and care. Because of them, I can concentrate more in my study without need to worry financial difficulties. Without them, it will be very difficult for me to come and study in Korea.

Finally, I would like to thank my parents, brother, relatives and friends for giving support and courage. Also thanks to Ko Antt Htet Wai for all the help and support .I greatly appreciate them and I will try my best to be a better and outstanding person .Thank you very much to you all.

Appendixes

Appendix A: Optimization of Bow at 25 knots

Appendix B: Optimization of Stern at 25 knots

Appendix C: Optimization of Bow at 22 knots

Appendix D: Optimization of Stern at 22 knots

Appendix E: Optimization of Bow at two speed (Multi-Objective)

Appendix F: Optimization of Stern at two speed (Multi-Objective)

Appendix G: Set up All run File for OpenFOAM



Appendix A: Optimization of Bow at 25 knots

	Bulb Height	Bulb Length	Bulb Width	Bulb Tangent angel	Entrance angle	Resistance
Dakota des001	4.30E-03	3.90E-03	-3.67E-04	-1.11E+01	-9.48E+00	15.056576
Dakota des002	4.99E-03	-3.35E-05	-7.46E-04	-1.50E+01	1.55E+00	15.894735
Dakota des003	4.99E-03	5.99E-04	1.49E-04	-6.84E+00	-2.80E+00	15.926297
Dakota des004	4.11E-03	4.87E-03	-4.97E-05	-3.10E+00	-4.15E+00	15.210652
Dakota des005	4.98E-03	1.79E-04	1.12E-04	-8.79E+00	7.48E-01	15.459226
Dakota des006	5.25E-04	4.25E-04	1.63E-04	-1.50E+01	-2.31E+00	15.935861
Dakota des007	4.97E-03	1.87E-04	1.04E-04	-8.60E+00	7.02E-01	15.121103
Dakota des008	3.70E-04	4.78E-04	1.54E-04	-1.49E+01	-1.98E+00	15.912593
Dakota des009	4.95E-03	2.43E-04	1.36E-04	-9.67E+00	1.12E+00	15.258454
Dakota des010	-5.33E-04	5.88E-04	1.93E-04	-9.87E+00	-3.77E+00	15.149278
Dakota des011	4.99E-03	-4.14E-06	3.04E-04	-7.72E+00	2.11E-01	15.213228
Dakota des012	5.01E-04	4.36E-04	1.50E-04	-1.50E+01	-1.55E+00	16.198364
Dakota des013	4.99E-03	7.17E-05	3.40E-04	-8.70E+00	2.31E-01	15.616375
Dakota des014	7.24E-04	5.08E-04	1.21E-04	-1.49E+01	-2.15E+00	16.122262
Dakota des015	4.95E-03	7.62E-05	1.06E-04	-9.02E+00	7.01E-01	15.430053
Dakota des016	4.21E-04	4.91E-04	1.68E-04	-1.50E+01	-2.40E+00	16.552842
Dakota des017	4.98E-03	1.91E-04	1.26E-04	-9.22E+00	7.19E-01	15.596629
Dakota des018	5.26E-04	4.91E-04	1.93E-04	-1.50E+01	-2.12E+00	16.325885
Dakota des019	4.98E-03	-1.65E-05	1.29E-04	-9.26E+00	9.09E-01	15.217032
Dakota des020	4.68E-04	5.39E-04	1.65E-04	-1.50E+01	-2.34E+00	16.772572
Dakota des021	4.97E-03	3.56E-04	9.73E-05	-9.16E+00	1.07E+00	15.464356
Dakota des022	4.22E-04	4.60E-04	1.78E-04	-1.50E+01	-2.51E+00	16.063411
Dakota des023	4.94E-03	1.61E-04	1.12E-04	-9.23E+00	8.37E-01	15.127688
Dakota des024	4.77E-04	5.75E-04	1.53E-04	-1.49E+01	-2.83E+00	16.054677

Dakota des025	4.96E-03	2.60E-04	1.20E-04	-9.30E+00	6.68E-01	15.332528
Dakota des026	5.52E-04	5.09E-04	1.67E-04	-1.46E+01	-2.91E+00	15.922486
Dakota des027	5.00E-03	8.54E-05	9.98E-05	-8.96E+00	6.36E-01	15.405269
Dakota des028	3.98E-04	4.64E-04	1.95E-04	-1.49E+01	-2.51E+00	15.935062
Dakota des029	5.00E-03	7.14E-05	8.04E-05	-9.44E+00	1.10E+00	15.169222
Dakota des030	4.76E-04	5.51E-04	1.77E-04	-1.49E+01	-2.86E+00	16.351742
Dakota des031	4.99E-03	1.36E-04	1.18E-04	-9.32E+00	1.17E+00	15.328691
Dakota des032	5.86E-04	4.15E-04	1.71E-04	-1.49E+01	-2.74E+00	16.181621
Dakota des033	5.00E-03	1.75E-04	1.18E-04	-9.14E+00	5.40E-01	15.278766
Dakota des034	4.78E-04	4.63E-04	1.56E-04	-1.50E+01	-2.48E+00	16.238622
Dakota des035	4.94E-03	2.70E-04	8.08E-05	-9.18E+00	4.96E-01	15.332863
Dakota des036	4.18E-04	5.16E-04	1.59E-04	-1.49E+01	-2.30E+00	16.645353
Dakota des037	4.98E-03	1.42E-04	5.88E-05	-9.22E+00	8.84E-01	15.194222
Dakota des038	4.89E-04	5.13E-04	1.41E-04	-1.50E+01	-2.50E+00	15.709273
Dakota des039	4.95E-03	2.52E-04	9.95E-05	-9.23E+00	8.26E-01	15.615156
Dakota des040	4.76E-04	4.87E-04	1.66E-04	-1.50E+01	-2.80E+00	15.746809
Dakota des041	4.99E-03	2.80E-04	1.05E-04	-9.09E+00	7.63E-01	15.406058
Dakota des042	3.71E-04	5.20E-04	1.58E-04	-1.49E+01	-2.19E+00	15.991581
Dakota des043	4.99E-03	9.60E-05	1.14E-04	-9.30E+00	8.71E-01	15.557532
Dakota des044	5.11E-04	4.61E-04	1.95E-04	-1.49E+01	-2.67E+00	16.654673
Dakota des045	4.99E-03	2.28E-05	9.33E-05	-9.49E+00	1.37E+00	15.279336
Dakota des046	-4.23E-04	5.97E-04	1.67E-04	-1.01E+01	-4.09E+00	15.043698
Dakota des047	4.97E-03	-8.47E-05	3.39E-04	-7.60E+00	3.20E-01	15.271299
Dakota des048	5.05E-04	4.10E-04	1.49E-04	-1.50E+01	-1.42E+00	15.793958
Dakota des049	4.97E-03	2.63E-04	3.90E-04	-8.62E+00	4.93E-01	15.273759
Dakota des050	6.43E-04	4.47E-04	8.85E-05	-1.50E+01	-2.10E+00	17.034835

Appendix B: Optimization of Stern at 25 knots

	Transom Height(d)	Resistance
Dakota_06_des0001	0.0000E+00	15.155748
Dakota_06_des0002	6.0000E-03	14.877845
Dakota_06_des0003	1.2000E-02	15.005545
Dakota_06_des0004	3.0000E-03	15.043436
Dakota_06_des0005	7.5000E-03	15.409805
Dakota_06_des0006	5.2500E-03	15.152359
Dakota_06_des0007	6.3750E-03	15.337906
Dakota_06_des0008	5.8125E-03	15.323031
Dakota_06_des0009	6.0938E-03	15.060946
Dakota_06_des0010	5.9531E-03	15.171683
Dakota_06_des0011	6.0234E-03	15.092281
Dakota_06_des0012	5.9883E-03	15.369809
Dakota_06_des0013	6.0060E-03	14.986436
Dakota_06_des0014	3.0000E-04	15.000128
Dakota_06_des0015	6.0000E-04	15.074541
Dakota_06_des0016	9.0000E-04	15.250012
Dakota_06_des0017	1.5000E-03	14.845122
Dakota_06_des0018	2.1000E-03	15.118934
Dakota_06_des0019	3.3000E-03	15.067575
Dakota_06_des0020	4.5000E-03	15.135761
Dakota_06_des0021	6.9000E-03	14.963473
Dakota_06_des0022	9.3000E-03	14.655671
Dakota_06_des0023	1.4100E-02	15.116071

Dakota_06_des0024	1.8900E-02	15.031248
Dakota_06_des0025	2.8500E-02	15.315763
Dakota_06_des0026	6.0000E-03	14.877845
Dakota_06_des0027	1.2000E-02	15.005545
Dakota_06_des0028	9.0000E-03	15.130077
Dakota_06_des0029	4.5000E-03	15.135762
Dakota_06_des0030	6.7500E-03	14.981685
Dakota_06_des0031	5.6250E-03	15.521095
Dakota_06_des0032	6.1875E-03	14.991348
Dakota_06_des0033	5.9063E-03	15.256185
Dakota_06_des0034	6.0469E-03	14.691714
Dakota_06_des0035	6.0938E-03	15.060946
Dakota_06_des0036	6.0703E-03	14.980171
Dakota_06_des0037	6.0352E-03	15.149018
Dakota_06_des0038	6.0529E-03	14.744426
Dakota_06_des0039	7.5685E-03	14.949668
Dakota_06_des0040	-7.3181E-03	15.616748
Dakota_06_des0041	-2.2035E-03	15.062669
Dakota_06_des0042	2.0207E-02	15.346672
Dakota_06_des0043	-1.8845E-02	15.435994
Dakota_06_des0044	7.8318E-03	14.979124
Dakota_06_des0045	3.1554E-03	14.981355
Dakota_06_des0046	8.4339E-03	15.430331
Dakota_06_des0047	5.4869E-03	15.536471
Dakota_06_des0048	9.0651E-03	15.332107
Dakota_06_des0049	5.8073E-03	15.224653
Dakota_06_des0050	8.9888E-03	15.565425

Appendix C: Optimization of Bow at 22 knots

Name	Bulb Height	Bulb Length	Bulb Width	Bulb Tangent angel	Entrance angle	Resistance
Dakota_09_des0001	0	0	0	0	0	12.127013
Dakota_09_des0002	1.00E-03	0	0	0	0	11.94887
Dakota_09_des0003	1.00E-03	1.00E-03	0	0	0	12.009054
Dakota_09_des0004	1.00E-03	0.00E+00	2.00E-04	0	0	11.926307
Dakota_09_des0005	1.00E-03	0.00E+00	2.00E-04	3.00E+00	0	12.245134
Dakota_09_des0006	1.00E-03	0.00E+00	2.00E-04	0.00E+00	3.00E+00	11.984261
Dakota_09_des0007	1.47E-03	-1.60E-04	2.12E-04	-2.55E+00	-4.64E-01	11.407417
Dakota_09_des0008	2.30E-03	-2.64E-04	2.20E-04	-4.19E+00	-7.62E-01	12.088883
Dakota_09_des0009	7.16E-04	-1.84E-04	2.14E-04	-4.50E+00	-5.31E-01	12.537526
Dakota_09_des0010	1.48E-03	-1.71E-04	2.68E-04	-1.65E+00	-1.32E+00	11.341264
Dakota_09_des0011	1.46E-03	-4.08E-04	2.10E-04	-2.48E+00	-3.97E-01	11.430981
Dakota_09_des0012	1.51E-03	2.76E-04	2.20E-04	-2.72E+00	2.29E-01	12.192822
Dakota_09_des0013	8.90E-04	2.11E-05	1.96E-04	1.56E-01	8.63E-04	11.935874
Dakota_09_des0014	9.76E-04	4.72E-06	1.99E-04	-1.71E-01	-4.95E-03	12.633681
Dakota_09_des0015	1.01E-03	3.07E-05	2.00E-04	1.10E-04	-2.30E-04	11.919605
Dakota_09_des0016	1.03E-03	-4.23E-06	1.99E-04	1.67E-01	-1.57E-03	11.983282
Dakota_09_des0017	9.96E-04	5.07E-06	1.96E-04	-6.52E-02	-1.10E-02	11.943389
Dakota_09_des0018	1.01E-03	-1.15E-06	2.00E-04	-9.02E-03	4.21E-02	12.024526
Dakota_09_des0019	1.47E-03	-1.60E-04	2.12E-04	-2.55E+00	-4.64E-01	11.407417
Dakota_09_des0020	1.41E-03	-5.16E-05	2.04E-04	-8.20E-01	-1.49E-01	11.272609
Dakota_09_des0021	1.03E-03	2.48E-04	2.00E-04	0.00E+00	0.00E+00	11.869332
Dakota_09_des0022	1.49E-03	2.04E-05	2.02E-04	-3.38E-01	-6.16E-02	12.016427

Dakota_09_des0023	9.33E-04	2.14E-05	2.00E-04	-7.19E-01	-9.83E-03	12.070928
Dakota_09_des0024	1.00E-03	-5.75E-07	2.00E-04	-9.13E-03	3.75E-01	11.94618
Dakota_09_des0025	9.81E-04	8.45E-05	2.02E-04	6.87E-01	-1.51E-01	11.947156
Dakota_09_des0026	9.88E-04	1.54E-06	1.75E-04	8.75E-03	1.59E-03	11.798969
Dakota_09_des0027	1.21E-03	-1.08E-06	1.73E-04	2.07E-02	-7.51E-02	12.550418
Dakota_09_des0028	9.93E-04	1.40E-06	2.00E-04	5.88E-03	-9.58E-03	11.870767
Dakota_09_des0029	1.00E-03	3.64E-06	2.00E-04	-6.75E-04	-2.49E-03	11.987818
Dakota_09_des0030	1.19E-03	-4.61E-03	8.50E-04	1.48E+00	3.74E-01	12.249463
Dakota_09_des0031	-1.38E-03	-3.20E-03	-5.26E-04	1.62E+00	2.08E+00	11.872573
Dakota_09_des0032	-3.00E-03	-2.87E-04	1.58E-04	-1.78E+00	-8.49E-02	11.883964
Dakota_09_des0033	-2.99E-03	-5.29E-05	1.58E-04	-1.19E+00	-1.67E+00	11.984095
Dakota_09_des0034	1.00E-03	-2.34E-07	2.01E-04	1.60E-02	4.70E-03	11.897302
Dakota_09_des0035	1.00E-03	5.11E-07	2.02E-04	3.65E-02	1.57E-02	11.946254
Dakota_09_des0036	9.98E-04	1.22E-06	1.99E-04	-7.96E-03	2.89E-03	11.911903
Dakota_09_des0037	9.97E-04	6.30E-07	2.00E-04	3.47E-03	-5.04E-03	11.870503
Dakota_09_des0038	-3.10E-03	-2.87E-04	1.58E-04	-1.79E+00	-8.49E-02	11.425761
Dakota_09_des0039	-1.27E-03	-5.30E-05	-5.25E-04	-1.20E+00	3.66E+00	12.682685
Dakota_09_des0040	1.47E-03	-6.04E-05	1.80E-04	-2.55E+00	-9.51E-01	11.360037
Dakota_09_des0041	1.49E-03	-2.04E-04	1.03E-04	-2.58E+00	-8.54E-02	11.372621
Dakota_09_des0042	1.33E-03	-7.74E-05	1.79E-04	-3.16E+00	-9.79E-01	11.406711
Dakota_09_des0043	1.55E-03	-1.34E-04	1.80E-04	-2.69E+00	-1.08E+00	11.314051
Dakota_09_des0044	1.69E-03	2.51E-05	1.82E-04	-3.02E+00	-8.31E-01	12.463119
Dakota_09_des0045	1.44E-03	-2.99E-04	1.76E-04	-2.36E+00	-1.38E+00	11.345013
Dakota_09_des0046	1.50E-03	-2.16E-04	1.78E-04	-2.52E+00	-1.23E+00	11.312795
Dakota_09_des0047	1.49E-03	-1.98E-04	1.87E-04	-2.52E+00	-1.34E+00	11.317438
Dakota_09_des0048	9.72E-04	6.03E-06	2.00E-04	3.11E-02	-2.62E-02	11.921722
Dakota_09_des0049	1.01E-03	-3.76E-07	2.02E-04	-1.59E-02	-8.33E-02	11.950961
Dakota_09_des0050	1.01E-03	-9.44E-07	1.98E-04	2.97E-02	-1.37E-02	11.919464

Appendix D: Optimization of Stern at 22 knots

	Transom height (d)	Resistance
Dakota_10_des0016	0.010327511	11.882632
Dakota_10_des0017	0.013327511	11.932417
Dakota_10_des0018	0.017827511	11.463812
Dakota_10_des0019	0.019327511	12.141157
Dakota_10_des0020	0.018577511	11.720569
Dakota_10_des0021	0.017452511	11.307974
Dakota_10_des0022	0.017077511	12.219269
Dakota_10_des0023	0.017640011	11.982471
Dakota_10_des0024	0.017358761	11.308271
Dakota_10_des0025	0.017499386	11.772479
Dakota_10_des0026	0.017429074	11.239247
Dakota_10_des0027	0.017405636	11.320928
Dakota_10_des0028	0.017440792	11.892045
Dakota_10_des0029	0.017423074	11.370678
Dakota_10_des0030	-0.011407678	12.250209
Dakota_10_des0031	-0.005407678	12.528157
Dakota_10_des0032	-0.017407678	12.030031
Dakota_10_des0033	-0.023407678	12.542303
Dakota_10_des0034	-0.014407678	11.884362
Dakota_10_des0035	-0.015907678	12.447729
Dakota_10_des0036	-0.013657678	12.113411
Dakota_10_des0037	-0.014782678	11.636929
Dakota_10_des0038	-0.015157678	11.720847

Dakota_10_des0039	-0.014970178	12.309898
Dakota_10_des0040	-0.014688928	11.984747
Dakota_10_des0041	-0.014829553	12.443223
Dakota_10_des0042	-0.014759241	11.395546
Dakota_10_des0043	-0.014735803	11.827622
Dakota_10_des0044	-0.014747522	11.655547
Dakota_10_des0045	-0.014765241	11.373822
Dakota_10_des0046	-0.014771241	11.354117
Dakota_10_des0047	-0.014777241	11.775727
Dakota_10_des0022	0.017077511	12.219269
Dakota_10_des0029	0.017423074	11.370678
Dakota_10_des0008	0.013615594	12.158296
Dakota_10_des0001	0.007803094	12.269701
Dakota_10_des0002	0.013803094	11.189808
Dakota_10_des0003	0.019803094	11.730282
Dakota_10_des0004	0.010803094	11.480576
Dakota_10_des0005	0.015303094	12.433643
Dakota_10_des0006	0.013053094	11.644005
Dakota_10_des0007	0.014178094	12.203031
Dakota_10_des0008	0.013615594	12.158296
Dakota_10_des0009	0.013896844	11.630268
Dakota_10_des0010	0.013756219	12.508218
Dakota_10_des0011	0.013826532	11.302042
Dakota_10_des0012	0.013791376	11.950925
Dakota_10_des0013	0.013809094	11.154795
Dakota_10_des0014	0.016327511	11.600497
Dakota_10_des0015	0.022327511	11.714839

Appendix E: Optimization of Bow at two speed (Multi-Objective)

	Bulb Height	Bulb Length	Bulb width	Bulb tangentangel	Entrance angle	Resistance1 (25 knots)	Resistance2 (22knots)
Geneticalgorithm_06_des0000	2.28E-05	3.39E-03	-3.44E-04	1.27E+01	-1.48E+01	15.629498	11.844312
Geneticalgorithm_06_des0001	-1.27E-03	-9.36E-04	-5.26E-04	1.03E+00	3.66E+00	15.249507	12.308469
Geneticalgorithm_06_des0002	-3.76E-03	1.66E-03	-3.28E-04	-1.25E+01	-6.95E+00	15.328219	12.138938
Geneticalgorithm_06_des0003	1.19E-03	-3.01E-03	4.71E-04	1.48E+00	2.86E-01	15.008436	11.824963
Geneticalgorithm_06_des0004	-3.10E-03	-5.29E-05	1.58E-04	-1.19E+00	-1.67E+00	15.512285	11.954164
Geneticalgorithm_06_des0005	-1.41E-03	-3.69E-03	2.61E-04	1.31E+01	-3.84E-01	15.111578	12.136563
Geneticalgorithm_06_des0006	1.82E-04	2.87E-03	8.51E-04	6.31E-01	-1.20E+01	15.178175	11.819636
Geneticalgorithm_06_des0007	6.54E-04	3.75E-05	-6.44E-04	1.49E+01	-4.00E+00	15.675247	11.833703
Geneticalgorithm_06_des0008	-3.09E-03	-5.29E-05	-5.26E-04	-1.66E+00	-1.73E+00	15.032388	12.045668
Geneticalgorithm_06_des0009	-1.27E-03	-9.33E-04	1.58E-04	1.50E+00	3.72E+00	15.484366	12.241667
Geneticalgorithm_06_des0010	1.18E-03	-3.01E-03	3.50E-04	1.48E+00	2.57E-01	15.092833	11.764109
Geneticalgorithm_06_des0011	1.92E-04	2.87E-03	9.72E-04	6.31E-01	-1.20E+01	15.141399	11.831898
Geneticalgorithm_06_des0012	1.81E-04	4.47E-03	4.72E-04	6.31E-01	-1.21E+01	15.268561	11.864062
Geneticalgorithm_06_des0013	1.19E-03	-4.61E-03	8.50E-04	1.48E+00	3.74E-01	15.600674	12.249463
Geneticalgorithm_06_des0014	-1.38E-03	-3.20E-03	-5.26E-04	1.62E+00	2.08E+00	15.109369	11.872573
Geneticalgorithm_06_des0015	-3.00E-03	-2.87E-04	1.58E-04	-1.78E+00	-8.49E-02	15.157291	11.883964
Geneticalgorithm_06_des0016	-2.99E-03	-5.29E-05	1.58E-04	-1.19E+00	-1.67E+00	15.379367	11.984095
Geneticalgorithm_06_des0017	-3.10E-03	-2.87E-04	1.58E-04	-1.79E+00	-8.49E-02	15.244371	11.425761
Geneticalgorithm_06_des0018	-1.27E-03	-5.30E-05	-5.25E-04	-1.20E+00	3.66E+00	15.490175	12.682685
Geneticalgorithm_06_des0019	-3.10E-03	-9.36E-04	1.57E-04	1.03E+00	-1.67E+00	15.186804	12.363214
Geneticalgorithm_06_des0020	-3.82E-03	-5.45E-04	-5.26E-04	1.48E+00	3.69E+00	15.49868	12.617154
Geneticalgorithm_06_des0021	3.73E-03	-3.40E-03	2.21E-04	1.03E+00	2.64E-01	15.923777	12.057691
Geneticalgorithm_06_des0022	-2.99E-03	-2.87E-04	1.58E-04	-6.00E+00	3.67E+00	15.435404	12.491535

Geneticalgorithm_06_des0023	-1.28E-03	-9.33E-04	1.65E-04	5.72E+00	-1.30E-02	15.426493	12.082605
Geneticalgorithm_06_des0024	-1.27E-03	-9.37E-04	-8.42E-04	-1.79E+00	3.67E+00	15.204213	11.934612
Geneticalgorithm_06_des0025	-3.10E-03	-2.86E-04	4.74E-04	1.03E+00	-8.58E-02	14.974409	11.794955
Geneticalgorithm_06_des0026	-3.10E-03	-2.92E-04	-5.26E-04	-1.79E+00	-8.49E-02	15.142021	11.911978
Geneticalgorithm_06_des0027	-1.27E-03	-9.31E-04	1.58E-04	1.00E+01	3.66E+00	14.953131	11.294335
Geneticalgorithm_06_des0028	-3.82E-03	-5.26E-04	-5.25E-04	5.39E-01	3.72E+00	15.070502	11.844988
Geneticalgorithm_06_des0029	-2.99E-03	-5.29E-05	1.57E-04	-2.55E-01	-1.70E+00	15.006219	12.125712
Geneticalgorithm_06_des0030	-2.57E-03	-5.45E-04	1.58E-04	1.03E+00	3.67E+00	15.142087	12.046894
Geneticalgorithm_06_des0031	-4.25E-03	4.69E-03	-5.26E-04	-1.34E+00	-5.32E-01	15.50544	12.387635
Geneticalgorithm_06_des0032	-2.16E-05	-9.36E-04	-5.92E-04	-1.40E+01	-8.54E-02	15.819941	12.344941
Geneticalgorithm_06_des0033	-4.25E-03	-2.87E-04	9.93E-05	-1.78E+00	3.67E+00	15.251406	12.087958
Geneticalgorithm_06_des0034	-4.11E-03	-2.33E-04	7.24E-04	1.48E+00	3.66E+00	15.432989	12.564037
Geneticalgorithm_06_des0035	-2.78E-03	-6.00E-04	-5.92E-04	-1.78E+00	-6.29E-02	15.325444	11.517649
Geneticalgorithm_06_des0036	-4.13E-03	-5.45E-04	-5.26E-04	1.03E+00	-1.18E+01	15.11429	11.830843
Geneticalgorithm_06_des0037	-2.78E-03	-2.87E-04	1.58E-04	-1.34E+00	1.49E+01	15.040436	11.176885
Geneticalgorithm_06_des0038	-1.43E-03	-9.32E-04	-8.42E-04	5.72E+00	3.66E+00	15.872591	12.343256
Geneticalgorithm_06_des0039	-2.83E-03	-2.92E-04	4.74E-04	-6.47E+00	-8.49E-02	15.107426	11.348564
Geneticalgorithm_06_des0040	-1.27E-03	-5.30E-05	-5.25E-04	-1.20E+00	3.66E+00	15.490175	12.682685
Geneticalgorithm_06_des0041	-3.10E-03	-9.36E-04	1.57E-04	1.03E+00	-1.67E+00	15.186804	12.363214
Geneticalgorithm_06_des0042	-3.82E-03	-5.45E-04	-5.26E-04	1.48E+00	3.69E+00	15.49868	12.617154
Geneticalgorithm_06_des0043	3.73E-03	-3.40E-03	2.21E-04	1.03E+00	2.64E-01	15.923777	12.057691
Geneticalgorithm_06_des0044	-2.99E-03	-2.87E-04	1.58E-04	-6.00E+00	3.67E+00	15.435404	12.491535
Geneticalgorithm_06_des0045	-1.28E-03	-9.33E-04	1.65E-04	5.72E+00	-1.30E-02	15.426493	12.082605
Geneticalgorithm_06_des0046	-1.27E-03	-9.37E-04	-8.42E-04	-1.79E+00	3.67E+00	15.204213	11.934612
Geneticalgorithm_06_des0047	-1.41E-03	-3.69E-03	2.61E-04	1.31E+01	-3.84E-01	15.111578	12.136563
Geneticalgorithm_06_des0048	1.82E-04	2.87E-03	8.51E-04	6.31E-01	-1.20E+01	15.178175	11.819636
Geneticalgorithm_06_des0049	6.54E-04	3.75E-05	-6.44E-04	1.49E+01	-4.00E+00	15.675247	11.833703
Geneticalgorithm_06_des0050	-3.09E-03	-5.29E-05	-5.26E-04	-1.66E+00	-1.73E+00	15.032388	12.045668

Appendix F: Optimization of Stern at two speed (Multi-Objective)

		Resistance1	Resistance2
	Transom Height(d)	25 knots	22 knots
Geneticalgorithmstern_09_des0000	0.009384	15.016435	11.830138
Geneticalgorithmstern_09_des0001	0.013792	15.484045	11.971599
Geneticalgorithmstern_09_des0002	-0.010079	15.418607	12.254679
Geneticalgorithmstern_09_des0003	-0.002269	15.096931	11.690503
Geneticalgorithmstern_09_des0004	-0.029654	15.921296	12.758231
Geneticalgorithmstern_09_des0005	0.012649	14.932161	11.278041
Geneticalgorithmstern_09_des0006	-0.011952	15.583361	12.218191
Geneticalgorithmstern_09_des0007	0.003557	15.210908	11.374246
Geneticalgorithmstern_09_des0008	0.016030	15.272098	12.039363
Geneticalgorithmstern_09_des0009	0.007329	15.282586	11.852598
Geneticalgorithmstern_09_des0010	-0.025788	16.546987	13.054802
Geneticalgorithmstern_09_des0011	0.027495	15.690444	11.436603
Geneticalgorithmstern_09_des0012	-0.010238	17.249143	14.149429
Geneticalgorithmstern_09_des0013	-0.002110	14.968771	11.336565
Geneticalgorithmstern_09_des0014	-0.002269	15.096931	11.690503
Geneticalgorithmstern_09_des0015	0.007329	15.282586	11.852598
Geneticalgorithmstern_09_des0016	0.001704	14.994871	11.241352
Geneticalgorithmstern_09_des0017	0.021772	15.247075	11.972454
Geneticalgorithmstern_09_des0018	0.012640	14.903708	11.324671
Geneticalgorithmstern_09_des0019	0.003566	15.250851	11.408285
Geneticalgorithmstern_09_des0020	0.014808	15.301839	12.245879
Geneticalgorithmstern_09_des0021	0.001398	15.243467	13.013387
Geneticalgorithmstern_09_des0022	0.015946	15.726241	12.123397
Geneticalgorithmstern_09_des0023	0.009468	15.327742	11.235557

Geneticalgorithmstern_09_des0024	-0.017344	16.595631	12.560744
Geneticalgorithmstern_09_des0025	0.027883	15.285322	12.079954
Geneticalgorithmstern_09_des0026	0.027488	15.803854	11.706906
Geneticalgorithmstern_09_des0027	0.009475	15.416821	11.297121
Geneticalgorithmstern_09_des0028	0.009475	15.416821	11.297121
Geneticalgorithmstern_09_des0029	0.014507	15.096514	11.784623
Geneticalgorithmstern_09_des0030	0.001649	15.625387	12.154299
Geneticalgorithmstern_09_des0031	0.009439	15.299587	11.365051
Geneticalgorithmstern_09_des0032	0.001704	14.994871	11.241352
Geneticalgorithmstern_09_des0033	-0.002269	15.096931	11.690503
Geneticalgorithmstern_09_des0034	-0.017359	16.702567	12.567907
Geneticalgorithmstern_09_des0035	0.027888	15.310361	12.110482
Geneticalgorithmstern_09_des0036	0.012647	14.970190	11.178562
Geneticalgorithmstern_09_des0037	0.009477	15.217756	11.279581
Geneticalgorithmstern_09_des0038	0.001704	14.994871	11.241352
Geneticalgorithmstern_09_des0039	0.009468	15.327741	11.235557
Geneticalgorithmstern_09_des0040	0.001631	15.527381	12.095632
Geneticalgorithmstern_09_des0041	-0.002095	15.555754	11.982712
Geneticalgorithmstern_09_des0042	0.012649	14.932161	11.278041
Geneticalgorithmstern_09_des0043	0.027640	15.554608	11.445459
Geneticalgorithmstern_09_des0044	0.012640	14.903708	11.324671
Geneticalgorithmstern_09_des0045	0.001704	14.994871	11.241352
Geneticalgorithmstern_09_des0046	0.001741	14.826331	12.146893
Geneticalgorithmstern_09_des0047	0.009439	15.299587	11.365051
Geneticalgorithmstern_09_des0048	0.012998	15.192567	12.146463
Geneticalgorithmstern_09_des0049	-0.028611	15.909408	12.681191
Geneticalgorithmstern_09_des0050	0.012890	14.963105	11.904277

Appendix G: Set up All run File for OpenFOAM

```
#!/bin/sh
cd ${0%/*} || exit 1 # Run from this directory
wmUNSET
source /opt/OpenFOAM-dev/etc/bashrc
touch case.foam
# Source tutorial run functions
. $Wm_PROJECT_DIR/bin/tools/RunFunctions
runApplication surfaceFeatureExtract
runApplication blockMesh
for i in 1 2 3 4 5 6
do
    runApplication -s $i \
        topoSet -dict system/topoSetDict.${i}

    runApplication -s $i \
        refineMesh -dict system/refineMeshDict -overwrite
done

runApplication snappyHexMesh -overwrite
runApplication setFields
runApplication decomposePar
runParallel renumberMesh -overwrite
runParallel $(getApplication)
runApplication reconstructPar
```